DISS. ETH No. 28118

PCR diagnostics within minutes: Assay development and optimization

A thesis submitted to attain the degree of

DOCTOR OF SCIENCES of ETH Zurich

(Dr. sc. ETH Zurich)

presented by

PHILIPPE BECHTOLD

MSc ETH Chemical- and Bioengineering, ETH Zürich

Born on 18.03.1995

Citizen of Luxembourg

Accepted on the recommendation of

Prof. Dr. Wendelin J. Stark, examiner

Prof. Dr. Paolo Arosio, co-examiner

2022

To my family

I'm a great believer in luck, and I find the harder I work the more I have of it.

(Thomas Jefferson)

Acknowledgements

My PhD has been a tremendous time of hard work, personal growth and even though it had ups and downs, I have thoroughly enjoyed it. The one person that made it possible was of course Prof. Wendelin Stark to whom I am sincerely grateful for the opportunity, the patience and the mentoring that made me progress that much. I want to also thank a person which has been on my side from before the PhD, Michele Gregorini. There have not been many days in the past 4 years that we have not discussed, planned, or decided anything and the journey we have embarked on has given my time at FML a special something.

I would not be in the privileged position I am now without my family. Thank you Mom and Dad for dealing with me since 26 years and shaping me into the adult I am now with all the support I could ever have wished for. Also thank you to Pit for supporting me in my sometimes basic struggles. In the same breath I wish to thank Rebecca, my partner in crime for being my rock and for filling up my energy stores with all the great things we do together.

My two lab mates for the better part of 3 years, Linda and Philipp, deserve a big thank you for the support, the discussions about science, life and everything else. The rest of FML also deserves recognition for the great community we have been. Thank you to Robert for the help with publications and extractions, thank you Urs, Oli, Julian, Simon, Anne, Patrick, Konsti for the continuously fun discussions and scientific exchanges. Thank you Niki for all the help and support in various challenges I encountered. Thanks to all the people who have already graduated and who have been examples for me in my first months. I have supervised more than 20 students during my time and want to thank all of you for working with me, pushing me harder and ultimately developing a great new technology. Thanks also to Mathias for the continuous support in my role as IT-admin of the group.

Since the beginning of my last year at FML, we have started onboarding people to especially help the development of peakPCR. I want to thank every single one of you: Amalia, Edgar, Viviane, Luca, Tobi, Thomas, Dario and Maria for committing to this adventure and for enriching my days at work and beyond.

A special shoutout goes to my Canadian family of whom I often think and from which learnings I made more than 10 years ago, I still benefit.

I could not have dealt with all the hardship of a PhD if I didn't have a place to vent. Sports have always been one of these places and therefore I would like to thank my teammates at the AECZ for the great atmosphere and for easing my integration into Switzerland. Another thanks needs to go to all the people I regularly cycle with, especially Joe and Simon for the joint suffering and stupidly hard rides we engaged in together.

Thanks to everyone I have interacted with in the last years as without discussions and confrontation with different views, one cannot develop professionally nor personally.

Table of Contents

Zusammenfassung

Die Erfindung der Polymerase-Kettenreaktion (PCR) vor mehr als 30 Jahren hat die Entwicklung einer enormen Vielfalt biotechnologischer Fortschritte ausgelöst. Deren Anwendungen reichen von der Gentechnik über die DNA-Sequenzierung bis hin zur Diagnostik. Im Laufe der Geschichte wurden die meisten wichtigen Erfindungen einem größeren Teil der Bevölkerung zugänglich gemacht. Die PCR ist eine der Erfindungen, die die breite Öffentlichkeit immer noch nicht erreicht hat und immer noch auf hochspezialisierte Labors in meistens Industrieländern beschränkt ist. Im Labor für funktionelle Materialien haben wir uns vorgenommen, diese Barriere der Unzugänglichkeit zu überwinden und haben ein PCR-Gerät entwickelt, das potenziell in größerem Maßstab von einer breiteren Öffentlichkeit genutzt werden könnte. In dieser Arbeit werden einige mögliche Anwendungen der Technologie in den Händen verschiedener Nutzer vorgestellt und die Vielseitigkeit des PCR Gerätes in verschiedenen Bereichen hervorgehoben.

In **Kapitel 1** wird eine allgemeine Einführung in die Geschichte der PCR und der DNA-Technologien gegeben. Ein ausgiebige Erklärung der Mechanik der PCR und der verschiedenen Nachweistechnologien legt dar, warum die PCR ein solch leistungsfähiges Werkzeug ist. Die verschiedenen Anwendungen der sehr vielseitigen Technologie werden mit besonderem Augenmerk auf die Bereiche erläutert, die am meisten von einem schnellen PCR-Gerät profitieren. Ausführlicher wird der diagnostische Anwendungsbereich beschrieben, da es sich hierbei um den momentan wichtigsten Einsatzbereich der PCR handelt.

Kapitel 2 behandelt eine klinische Studie, die ich mit mehr als 250 Personen während der COVID-19-Pandemie durchgeführt habe. Ziel war es, herauszufinden, ob das von uns entwickelte schnelle PCR-Protokoll als PCR-Selbsttest verwendet werden kann. Diese Frage war zuvor nicht sehr oft gestellt worden, da PCR-Geräte für Laien unzugänglich waren. Die Ergebnisse waren ermutigend, da die meisten Personen ohne vorherige Schulung in der Lage waren, den PCR-Teil des Tests durchzuführen, während sich der präanalytische Schritt als verbesserungsbedürftig herausstellte.

Kapitel 3 steht ebenfalls im Zusammenhang mit der aktuellen Pandemie, da das Kapitel einen Test zum Nachweis der gefährlichen Mutationen von Sars-CoV-2 beschreibt, den ich zusammen mit dem Schweizerischen Tropeninstitut in Basel entwickelt habe. Anfang 2021 bestand ein erhöhter Bedarf an Kapazitäten zum Sequenzieren, um allfällige Mutationen von Sars-CoV-2 zu

überwachen. Wir haben einen PCR-basierten Assay entwickelt, der die wichtigsten Mutationen direkt am primären Testpunkt nachweisen kann. Der Assay wurde auf einer einzigen Kartusche unserer schnellen PCR-Plattform verpackt, so dass die wichtigsten Mutationen innerhalb von 40 Minuten nachgewiesen werden konnten. Die Resultate zeigten, dass die Leistung des Schnelltests vergleichbar ist mit der eines hochmodernen PCR-Geräts und die Spezifität der Tests bei 100 % liegt.

In **Kapitel 4** werden verschiedene diagnostische Tests für Malariaparasiten verglichen und ein 30-minütiger PCR-Test mit sehr hoher Empfindlichkeit und Spezifität vorgestellt. Zu den bestehenden Tests für *Plasmodium falciparum* gehören vor allem Schnelltests (RDT) auf der Grundlage der Lateral-Flow-Technologie. Leider werden bei den weit verbreiteten RDTs viele Fälle übersehen, genau wie bei der traditionellen Mikroskopie. Das von uns entwickelte PCR-Schnellverfahren dauert nur 30 Minuten und ist fast so sensitiv wie ein modernes Referenzverfahren, das jedoch in den meisten von Malaria betroffenen Gebieten nicht verfügbar ist. Zusammen mit der PCR Kartusche, die alle Reagenzien enthält und die ohne Kühlkette gelagert werden kann, könnte diese Entwicklung eine Point-of-Care Malaria-Diagnostik im Feld ermöglichen.

Summary

The invention of the polymerase chain reaction (PCR) more than 30 years ago has sparked the development of a tremendous variety of biotechnological advancements. Applications thereof range from genetic engineering to synthesis and to diagnostics. Over time, all major inventions have been made available to a larger portion of the population. PCR is one of those technologies which has not yet reached the wider public and is still constrained to highly specialized laboratories in mostly developed countries. At the Functional Materials Laboratory, we have set out to overcome this barrier of inaccessibility and have developed a PCR device that could at some point be used at a larger scale by a broader audience. This work presents some potential applications of the technology in the hands of different users and highlights the versatility of PCR in different settings.

In **Chapter 1**, a general introduction to the history of PCR and DNA technologies is laid out. A deep dive into the mechanics of PCR and the different detection technologies explains why PCR is such a powerful tool. The different applications of this versatile technology are explained with a special regard to those that could profit most from a rapid PCR device. More detail is put into the diagnostic field of application as it is the most impactful area of use of PCR nowadays.

Chapter 2 covers a clinical study that I performed with more than 250 people during the COVID-19 pandemic. The goal was to find out if the rapid PCR protocol we had designed was usable as a PCR self-test. This question has not been asked previously as PCR devices were inaccessible to laypeople until now. The results were encouraging as without prior training, most people were able to perform the PCR part of the test, while the pre-analytic step was shown to need improvement.

Chapter 3 is also in the context of the current pandemic as it describes an assay to detect the mutations of concern of Sars-Cov-2 that I developed together with the Swiss Tropical and Public Health Institute in Basel. There was a need for more sequencing capacities in early 2021 to monitor the mutations of Sars-CoV-2. We developed a PCR-based assay that can detect the most important mutations directly at the primary point of testing. The assay was packaged onto a single cartridge of our rapid PCR platform so that the most important mutations were detectable within 40 minutes. The performance of the rapid assay is similar to a state-of-the-art PCR device and the specificity of the test is 100%.

In **Chapter 4** various diagnostic tests for malaria parasites are compared and a 30-minute PCR assay with very high sensitivity and specificity is presented. The existing assays for *Plasmodium falciparum* include mostly rapid diagnostic tests (RDT) based on lateral-flow technology. Unfortunately, the widely used RDTs miss many cases, just like traditional microscopy. The rapid PCR procedure we have developed takes only 30 minutes and is almost as sensitive as a state-of-the-art reference which is however unavailable in most of the areas affected by malaria. Together with the consumable that contains all reagents and that is storable without requiring a cold-chain, this development could enable Point-of-Care malaria diagnostics in the field.

1. Polymerase Chain Reaction and its Applications

1.1. History of PCR

The research laid out in this work focuses on a variety of applications of polymerase chain reaction (PCR), namely the diagnosis of Sars-Cov-2 and its variants of concern as well as the diagnosis of malaria, a widespread tropical disease.

PCR, a method to multiply Deoxyribose Nucleic Acid (DNA) molecules, was discovered and patented in the late 70s and 80s after Watson and Crick laid the base for the understanding of the hereditary information carrier called DNA by elucidating its structure in 1953 [1]. Later Arthur Kronberg identified the first DNA Polymerase, the enzyme responsible for the synthesis of new DNA strands in 1957 [2]. Interestingly, he was awarded the Nobel Price before his peers, Watson and Crick, who discovered the structure of DNA itself (1959 vs 1962).

It took another 20 years until the first thermostable polymerase was isolated [3], which allowed for a less labor intensive procedure and is still in use today with only minor modifications [4].

In 1983 Kary Mullis invented the PCR as we know it today by adding an additional primer to the then relatively new Sanger sequencing [5]. The invention of PCR, which Mullis filed a patent for in 1987 earned him the Nobel Prize in 1993 [6].

Already in the 90s, the U.S. Food and Drug Administration (FDA) cleared the first PCR-based diagnostic test for use [7]. Within a few years, PCR replaced established tools such as viral and microbial culturing on plates from the inventory of clinical microbiology.

Molecular diagnostics is still evolving at an astonishing pace with new devices and methods being brought forward every year, especially during the current Sars-CoV-2 pandemic [8]. In order to understand the engineering involved in my work, it is essential to take a deeper look into the mechanics of the polymerase chain reaction.

1.2. How PCR works

The starting point of a PCR is always a strand of DNA. DNA is the hereditary material in all humans and most other organisms. The four nucleic bases that can be found in DNA are adenine (A), guanine (G), cytosine (C), and thymine (T) encoding the information used to create any form

of life and which is passed on through generations in the form of genes[1]. The nucleic bases form a nucleotide together with a sugar molecule and a phosphate molecule, as can be seen in Figure 1.

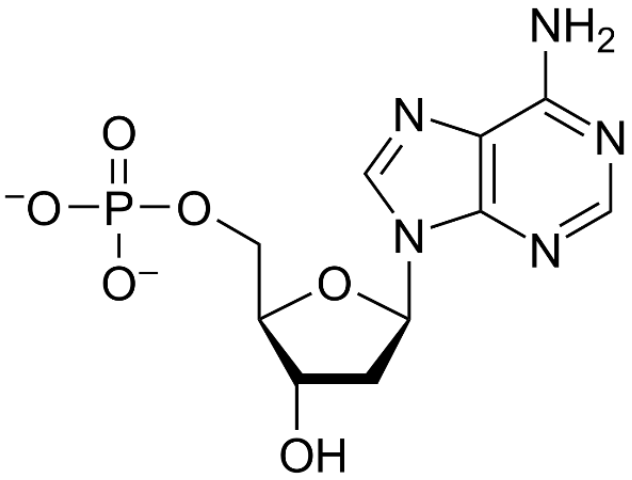

Figure 1. Chemical structure of a DNA nucleotide with an adenine base attached. The phosphate molecule is attached to the 5' position of the pentose.

[1] The words gene and generation have different etymological origins. Gene was coined by the Danish botanist Wilhelm Johannsen who was inspired from the greek word "*genos*", meaning birth [139]. Generation however originates from the latin "*generare*" meaning to bring forth or to produce and has been incorporated from the French "*generation*" which means race, people.

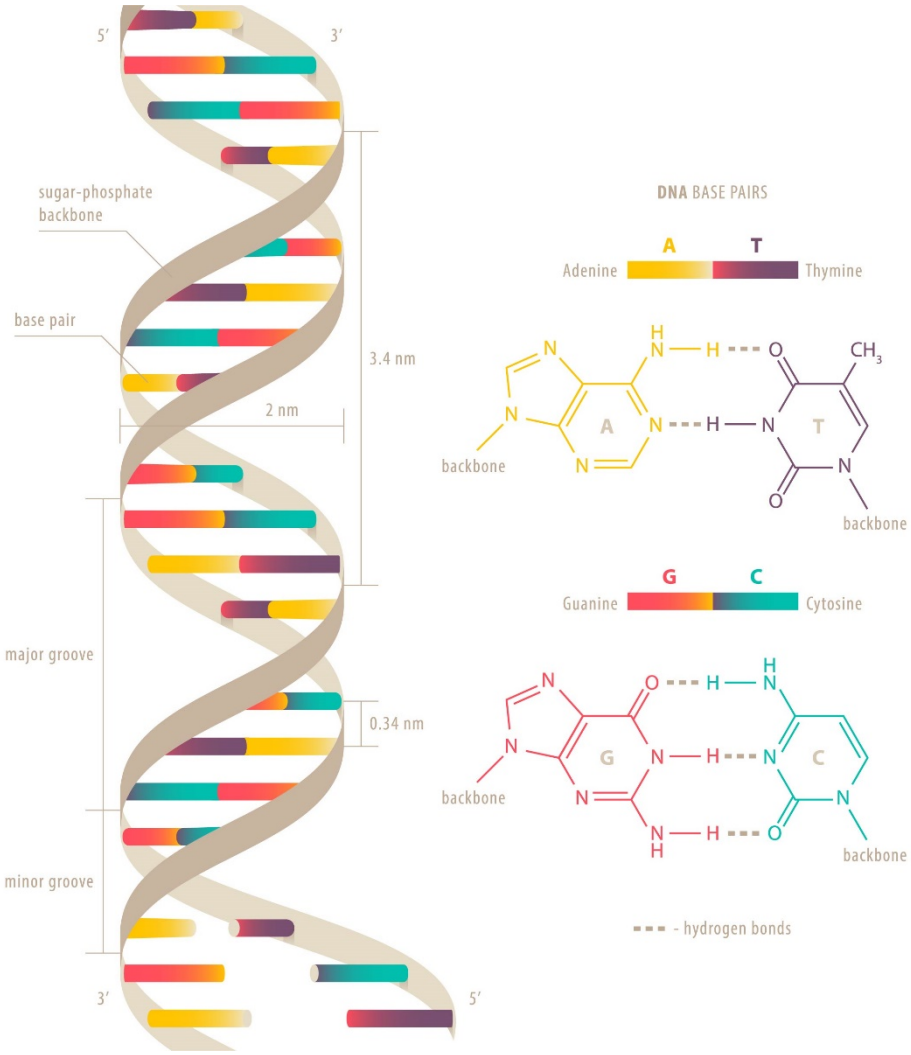

Figure 2. Double helix structure of DNA. On the right, the chemical structures of the four bases A, T, G and C are shown as well as the specific hydrogen bonds that only allow for A-T and G-C pairing know as Watson-crick pairing. Taken from [9].

Nucleotides can polymerize at the 5’ phosphate position and the 3’ OH position to form a the backbone of DNA (deoxyribose as a sugar) or RNA (ribose as sugar) strand as indicated in Figure 2.

DNA strands can be reverse complementary and form a double helix as seen in Figure 2. The double helix is called a double-stranded DNA (dsDNA). By convention the end with a phosphate termination is called 5’ and the end with an OH is named 3’. Going by convention, 5’ to 3’ states the forward translational direction.

A single molecule of DNA makes up a chromosome, which is circular in bacterial cells and X-shaped in eukaryotic and plant cells, depending on the phase in the cell cycle. The chromosome is

situated in the cell nucleus and, again depending on the cell phase can even be seen by light microscopy. The number of chromosomes as well as their size varies greatly between species.

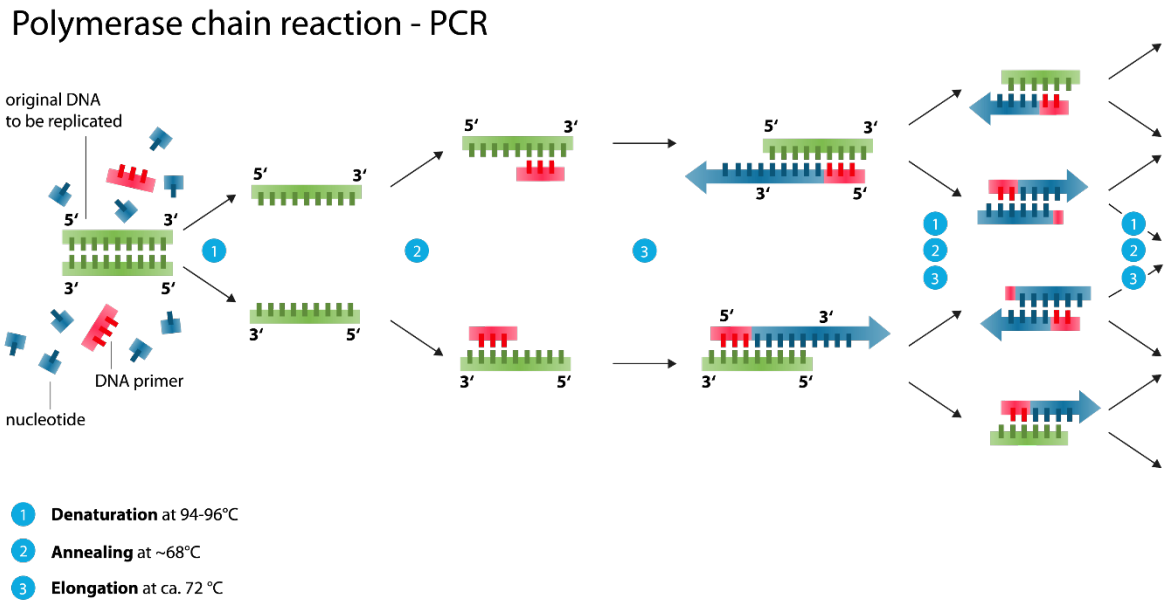

Figure 3. Polymerase chain reaction and the thermocycling steps. Taken from [11].

Once all reagents are mixed, the PCR is initiated by an initial denaturation step at around 95 °C which also activates the modern polymerase enzymes [12]. In Figure 3, this step is labeled as 1. By lowering the temperature to about 68 °C, the hydrogen bonds between the respective bases reform, leading to the annealing (=binding) of the primers to their complementary sequence. This is marked as step 2 in Figure 3. As the temperature increases to 72 °C, the polymerase reaches its peak activity, attaching to the primers and synthesizing the complementary strand of DNA in the 5’ to 3’ direction using the original strand as a template. The product at the end of the so-called

elongation period (step 3 in Figure 3) being a duplication of the amount of template present at the beginning. Repeating the temperature steps is called cycling leading to the exponential multiplication of DNA molecules. The products of PCR are further used for either high-throughput sequencing or biotechnological applications such as cloning or mutagenesis [13].

1.3. Quantitative PCR (qPCR)

The products of a PCR are not easily detected. The original technique, invented by A. Tiselius [14], uses gel electrophoresis where the DNA strands are stained with a fluorescent dye namely ethidium bromide (EtBr) and then separated over a gel under application of a voltage. The DNA is separated by length enabling the identification of the desired product when comparing it to a reference ladder [15]. EtBr is a DNA intercalating dye with a higher fluorescence when bound to dsDNA than when in solution [16]. Modern iterations of intercalating dyes include the SYBR family which are less carcinogenic and more sensitive [17]. SYBR Green I is also used in PCR mixes [18] to detect amplified DNA at the end of each extension phase during the PCR. This technique is called quantitative PCR (qPCR) because it allows for the quantification of the initial amount of template in the sample [19] through an external calibration.

For diagnostics, unspecific dyes like EtBr and SYBR do not offer the unambiguity needed for definitive answers at low template concentrations [20]. The solution is fluorescent probes that come in many variations [21]. The most commonly used probes are so-called TaqMan Probes first described 20 years ago [22].

In general, a probe is an oligonucleotide containing a fluorophore (such as 6-Carboxyfluorescein) on the 5’ end and a fluorescence quencher (such as BHQ) on the other end as shown in Figure 4. Probes add another layer of specificity as they only hybridize on the desired sequence. Another key advantage of using probes is multiplexing, that being the simultaneous amplification of multiple fragments with probes of different fluorescence spectra allowing for the discrimination of multiple analytes in a single reaction [23]. Due to the short nature of the oligonucleotides, the quencher effectively silences the signal emitted by the fluorophore. The technique makes use of the 5’ exonuclease activity of most polymerases that essentially disintegrates the oligonucleotide

and thereby releases the fluorophore removing the signal suppression of the quencher [24]. For each amplified strand, one fluorophore molecule is released into the reaction mix.

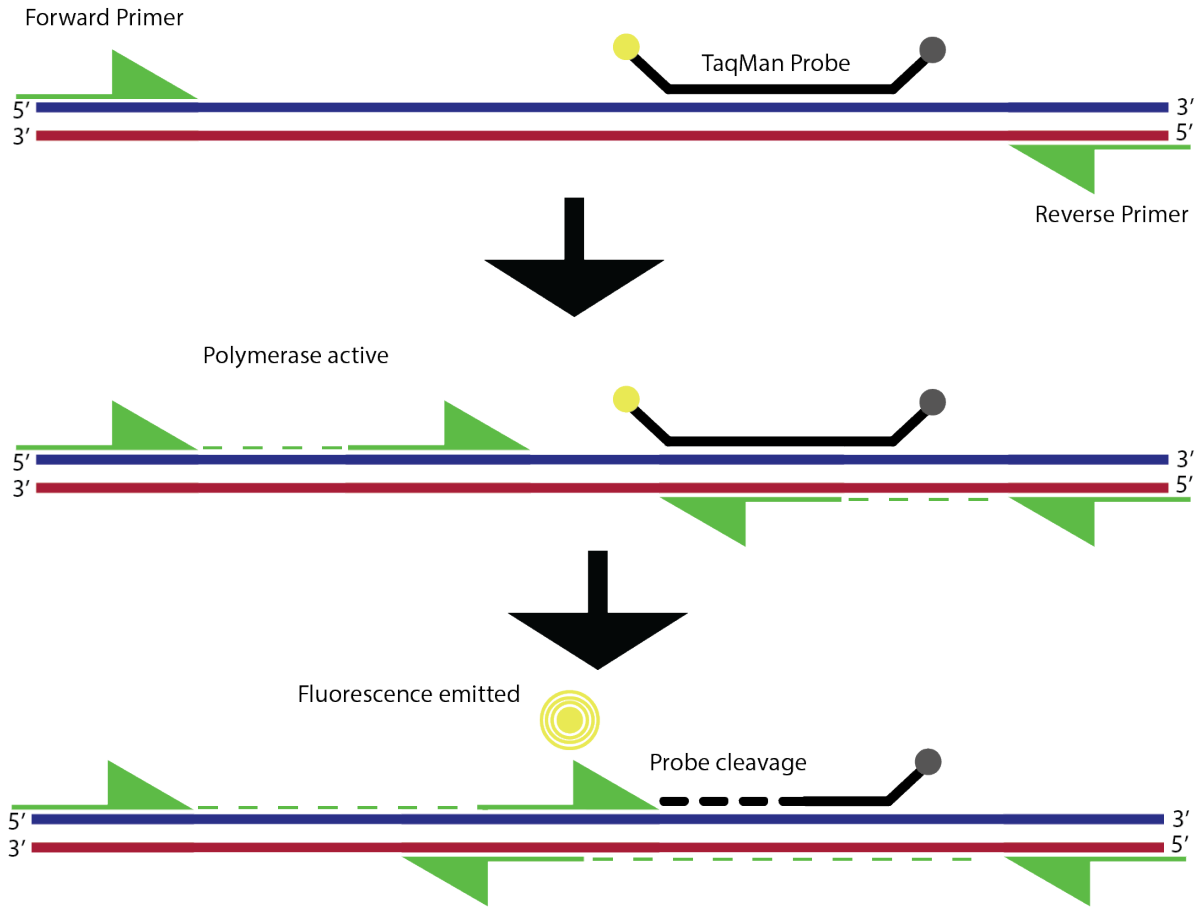

Figure 4. Schematics of the mechanism of action of a Taqman probe.

Over time, the fluorescence in the mix increases exponentially – just like the product - until it reaches a plateau which can be seen in Figure 5. The flattening of the curve is due to depletion of nucleotides, primers or inhibition of the polymerase due to the high DNA concentration [25]. The resulting sigmoidal curve can be fitted in many different ways [26], but the parameter used for quantification is most often the threshold cycle *Ct.* A lower *Ct* indicates a higher initial

concentration whereas a higher Ct indicates a lower initial concentration. In order to fully quantify how much template is present in a sample, a calibration curve is required.

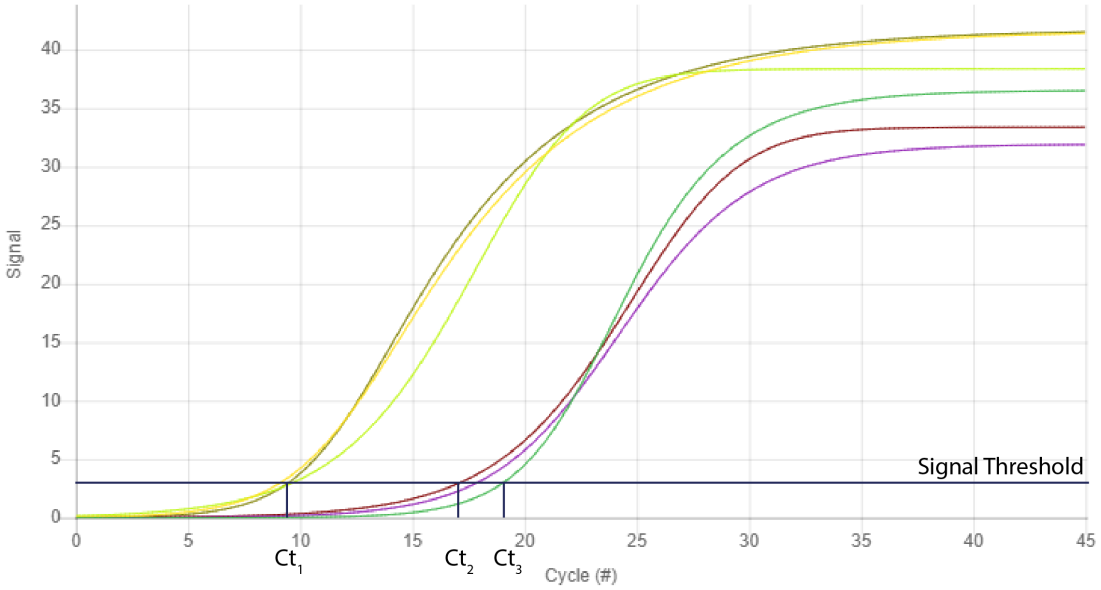

Figure 5. Amplification curves of a dilution curve of a PCR test for Schistosomiasis. The curves in the lighter colors have a higher concentration of analyte compared to the darker curves. Note that the shape or maximums of the curves are not of importance for quantification.

1.4. Reverse Transcriptase quantitative PCR (RT-qPCR)

DNA polymerase catalyzes the PCR reaction but can only use DNA as a starting material. As many organisms, especially viruses, carry RNA, instead of DNA, as hereditary material these organisms cannot be identified by classical qPCR. The solution is to add a reverse transcription step before the classical PCR to transcribe RNA into complementary DNA (cDNA) [27], [28]. cDNA can then be used as a template for qPCR. Modern master mixes already combine the reverse transcriptase and the PCR reagents in a single kit to allow for higher throughputs and less hands-on time [29].

1.5. Applications of qPCR

The applications of the qPCR technology are manifold and I want to give an overview of the four most relevant areas: gene expression monitoring, food safety and quality, genetically modified organisms (GMO) detection and human diagnostics.

1.5.1. Gene expression monitoring

One important application for RT-qPCR is the monitoring of gene expression levels in biological applications. Monitoring of gene expression levels comprises the analysis of differences induced by genetic modification, the characterization of the base expression levels of cell lines, the analysis of the reaction of certain cells to external or internal stresses [30] and the study of behaviors of certain expression pathways [31].

The three-step workflow in these four cases relies on the extraction of only RNA from the target cells. Firstly, it is important that all DNA is degraded to limit the quantification to the expression level. Secondly, the extracted mRNA is subsequently reverse transcribed into cDNA. In a third step, the qPCR step is performed on the fragments of interest [32]. Usually a reference gene, also called house-keeping gene, whose expression level is constant under the experiment conditions is also analyzed to allow for relative quantification [33]. The outcome of the experiments are the relative levels of genetic expressions, which can be linked to behaviors of the organism under analysis.

1.5.2. Food safety and quality

The identification of small quantities of pathogens in foodstuff has been a concern for many decades [34]. Already in the 80s, qPCR was utilized to detect and quantify enterohemorrhagic *E. coli* (EHEC) [35]. Other pathogens that are routinely detected with qPCR include *Salmonella enterica, Vibrio parahaemolyticus, Plesiomonas shigelloides and Listeria monocytogenes* [36].

Before a qPCR analysis can be performed, the sample (which may be a large amount of material, at least 100 g [37]), is enriched by culturing it overnight. Then DNA is extracted from the usually complex matrix and the qPCR is performed as usual [38]. Assays for foodstuff are heavily multiplexed and have high throughput. The prior state-of-the art was culturing of the organisms present in the samples, which is extremely time- and labor-intensive (see Figure 6). The qPCR workflow also requires the enrichment period in a liquid medium which takes many hours. Therefore, the overall time saved by a potentially faster PCR is not significant.

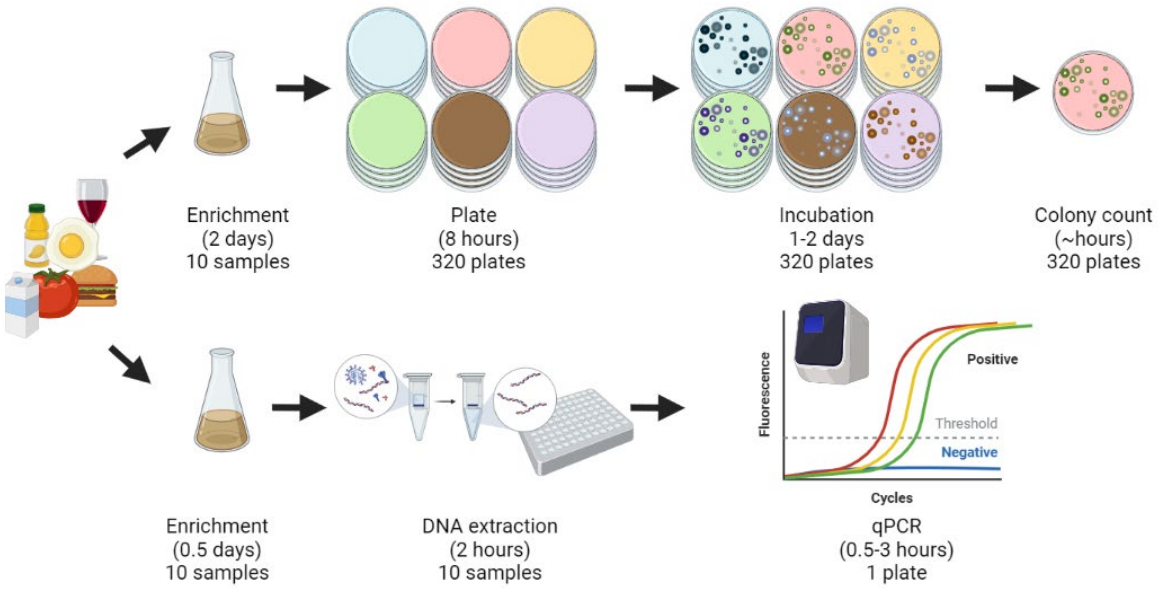

Figure 6. Comparison of traditional microbiological testing to qPCR methods with the example of foodstuff. Not only is qPCR significantly faster, but it also requires less labor-intensive steps. Furthermore, the extracted DNA is well storable and can be retested for other organisms of interest at a later point in time [39], [40].

1.5.3. GMO detection

A topic related to food safety is the quantification of the genetically modified organisms (GMO) content in crops. Globally, the most important GMO crops are soybean, maize and cotton [41]. In 2003, the European Union (EU) decided to limit the use of GMO in crops [42]. In 2013, they introduced a regulation to limit the GMO content of foodstuff to a maximum of 0.9% [43]. The state-of-the-art that is accepted by the EU is set up by the European Network of GMO Laboratories and is with only few exceptions qPCR [44]. The GMOs are detected through their transgenic elements, usually p35s or tNOS [45]. A special challenge is the correct establishment of a baseline, for which the EU has certified reference materials available that need to be extracted in parallel [46]. As the amount of inhibitors is naturally high, the extraction of pure DNA, needed for accurate quantification, is difficult and hard to execute outside of a highly equipped laboratory [47].

The challenging extraction with long hands-on time is a reason why a rapid PCR would also not be of great impact as most time is spent upstream of the actual detection. Although the decentralized application of PCR in soybean mills for example could be of great interest to reduce downtime caused by GMO contamination, the need for EU certified reference material in every single mill would render the effort humongous.

1.5.4. Diagnostics

Human diagnostics are used to indicate which disease a patient is suffering. There is a definitive improvement in the efficacy of the treatment of the disease if it can be identified correctly. In the case of infectious disease diagnostics, there is a manifold of approaches which can be classified into three main methods: either measuring the presence of an infectious agent directly, measuring the presence of an infectious agent indirectly (through presence of its genotype) or though the body's response to an infection. All of these technologies have developed into a manifold of different variations.

The most common diagnostic tests derived by the three methods mentioned are the antigen test, the antibody test and the RT-qPCR test respectively.

Antigen tests are based on the immunoassay principle that relies on the specific binding of an analyte to an antibody with the generation of a colorimetric signal for readout. Most commonly they are commercialized as lateral-flow devices [48] as can be seen in Figure 7. In these assays, the sample is suspended in a buffer and applied to a sample pad allowing for the sample to flow through the device. The labeled antibodies that are immobilized in the conjugate pad bind to the analyte and migrate down the assay due to capillary flow.

A lateral flow assay contains two lines, the test line and the control line, both are orthogonal to the flow direction. The test line caries the antibodies for the investigated analyte and the control line binds the antibodies with a tag giving the user a binary, yes/no output whether the test has worked or not. It is important to mention that a lateral-flow assay takes between 15 and 30 minutes to yield a result.

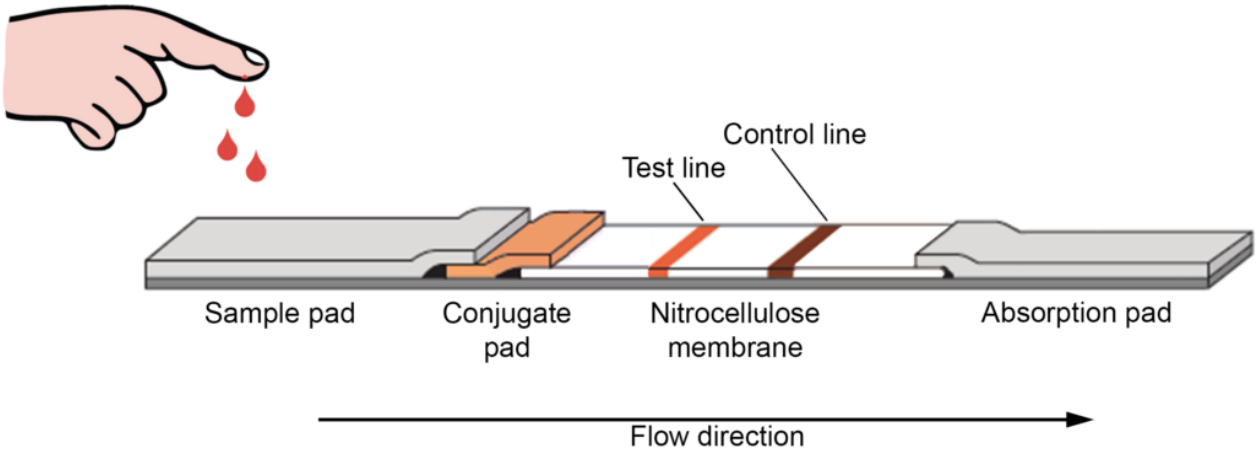

Figure 7. Schematics of a lateral flow assay. Image taken from [49]

In most diagnostic applications, the analytes are antigens of the pathogen. In the case of Sars-CoV-2 for example, the most used antigens are nucleocapsid-, spike-, envelope- or membrane proteins [49].

Antibody tests are also distributed as lateral-flow assays with the difference that the analyte is an antibody produced by the body as a response to an infection [50]. Thereby it is an indirect sign of an infection. Antibody tests can be used to check if an infection with a specific disease has previously occurred as antibodies have a long half-life in the body [51]. The presence of antibodies is also an indication if a vaccination has elicited a response from the immune system [52].

RT-qPCR has been described extensively in paragraph 1.4; in summary, it involves four steps: lysis of the sample to release the DNA, purification of the RNA, reverse transcription into cDNA and optical detection of the amplified cDNA. Before the primers for a diagnostic assay can be designed, the sequence of the pathogen needs to be sequenced. The choice of primers has a large influence on the performance of the assay [53], [54].

qPCR as a diagnostic tool has disadvantages compared to the Antigen and the Antibody test requiring an extraction step to yield relatively pure nucleic acids for it to detect low concentrations. Additionally, PCR is nowadays mainly used in centralized laboratories, adding a time- and resource-inefficient transportation step and delaying the start of the correct treatment [55]. Another issue reported about PCR as a diagnostic tool is the occurrence of false positives shortly after recovering from a disease. The positive result is caused by the target of PCR which

is a RNA/DNA sequence and may be present after the infectious agent has rendered inactive by the immune response [56].

The rapid spread of the current Sars-CoV-2 pandemic has introduced an enormous need for large-scale testing. However, the quality of the results of rapid tests is not high enough for efficiently fighting the pandemic [57], [58]. Especially in samples with low viral load, the sensitivity is drastically lower than in PCR testing [59].

Antibody tests are not very useful to detect a newly acquired infection as the bodies response of antibody production is delayed by around 4-5 days [60].

The gold-standard in diagnostics to detect an ongoing infection is still the nucleic acid amplification test. Although many different variants such as Loop-mediated isothemal amplification (LAMP), strand displacement amplification (SDA), recombinase polymerase amplification (RPA) and several others have been developed in recent years, PCR is analytically still outperforming them in most cases [61]–[64]. PCR has the advantage that the assay design is relatively simple requiring only two primers and the probe, whereas LAMP for example needs six primers. The strand displacement assays have the advantage that they may use enzymes able to tolerate inhibitors whereas Taq polymerases cannot. However the most sensitive molecular diagnostic assays rely on the inhibitor sensitive reverse transcriptase to detect both RNA and DNA from the target pathogen [65] and to thereby lower the limit-of-detection. In this work I show that with the correct instrumentation, inexpensive and simple PCR can be performed, performing better than other state-of-the-art techniques presented.

The significance of qPCR for diagnostics cannot be underestimated, it being the largest market for qPCR applications with revenues of about 9.7 Billion USD annually and growing with a rate of 9% annually [66] as shown in Figure 8.

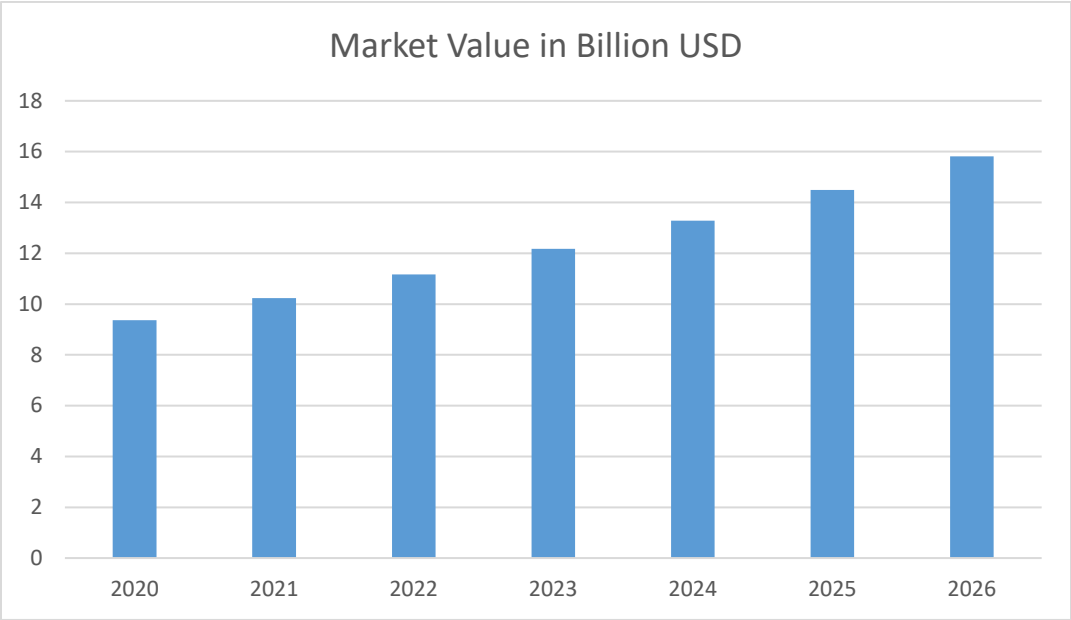

Figure 8. Forecast of the annual revenues of the molecular diagnostics market for the next 5 years.

Overall there is a continuing need for PCR diagnostics [67]; whether it be in central laboratories, at the Point-of-Care (PoC), in high-income countries or in low and medium income countries.

1.6. PCR in PoC settings

Traditionally, PCR was only available in large central laboratories because the PCR machines and its reagents are expensive, often designed for high-throughput applications and require extensive training to operate correctly. Another issue that limits the use of PCR in clinical laboratories is the slow reaction speed conventional thermocyclers offer, which allows a full 45 cycle PCR in only 1.5-2 hours. The need for highly trained personnel adds to the overall cost of the method, making it one of the most expensive diagnostic methods in the Swiss healthcare system [68]. The handling and cost of devices can be adapted to decentralized testing; however, the long reaction times are intrinsically linked to the heat transfer limitations of standard polymer tubes utilized by conventional PCR machines.

Point-of-Care (PoC) testing is defined as medical diagnostic testing at or near the patient and the time where care is required [69]. It has special requirements, as the test is not done in a laboratory and needs to be operated by a layperson. Furthermore, the result needs to be available within minutes [70]. PoC testing encompasses a great variety of analytes, ranging from hormones to

blood markers over to pathogens [71], like in the pregnancy test, the most successful PoC analysis on the market.

We have developed a device that can perform PCR within minutes and is therefore catered for such PoC applications. We have named it “peakPCR” and it is explained in detail in the following section.

1.7. The peakPCR rapid PCR system

peakPCR has been developed in the group of Prof. Wendelin Stark with the aim of making PCR faster and more accessible. It has shown to run a full PCR with 42 cycles in less than 10 minutes (unpublished work). The thermocycler is made from off the shelf components and therefore offers a low price of production [72]. The design features an absence of moving parts, significantly lowering the need of maintenance needed. Together with the cartridge, made of aluminum, enabling to contain all necessary reagents in a storable form, the platform is perfect for remote, in-the-field applications. The first iteration of the device, which was used for all experiments shown in this work can be seen in Figure 9.

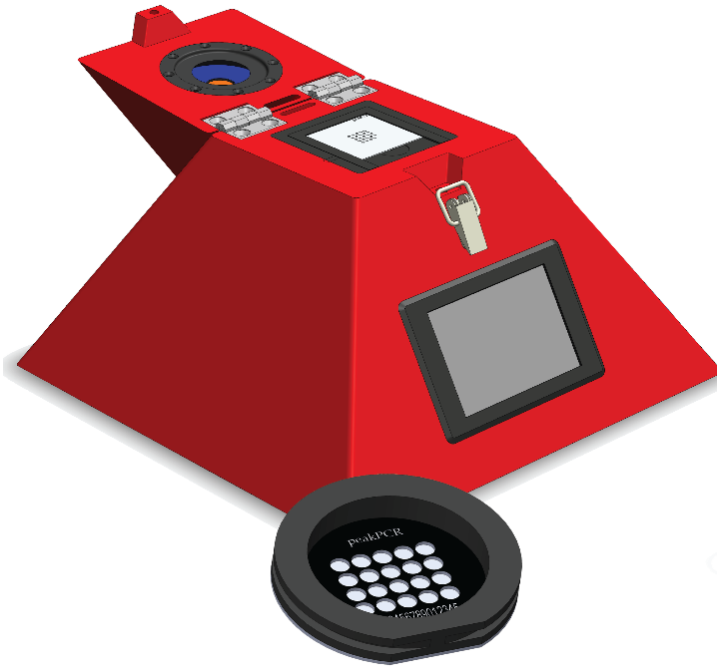

Figure 9. peakPCR device and a cartridge used for qPCR

In this dissertation, I lay out the different uses of the peakPCR system and show the flexibility of the diagnostic assays that can be performed. A first application was the self-testing of Sars-CoV-

2 that I investigated with a clinical study performed at ETH Zurich. Further on the topic of Sars-CoV-2, I worked with the Swiss Public and Tropical Health Institute (SwissTPH) on the detection of variants-of-concern of the virus [73] and finally I worked on an assay for tropical diseases and leveraged the peakPCR platforms ability to deliver sample-to-result answers in less than 30 minutes. I am delighted to present to you the work I have put into this dissertation in the last 3.5 years.

2. Video supervised COVID-19 self-testing on lean-design PCR machines: Transporting instruments instead of patients as a way to reduce viral spreading

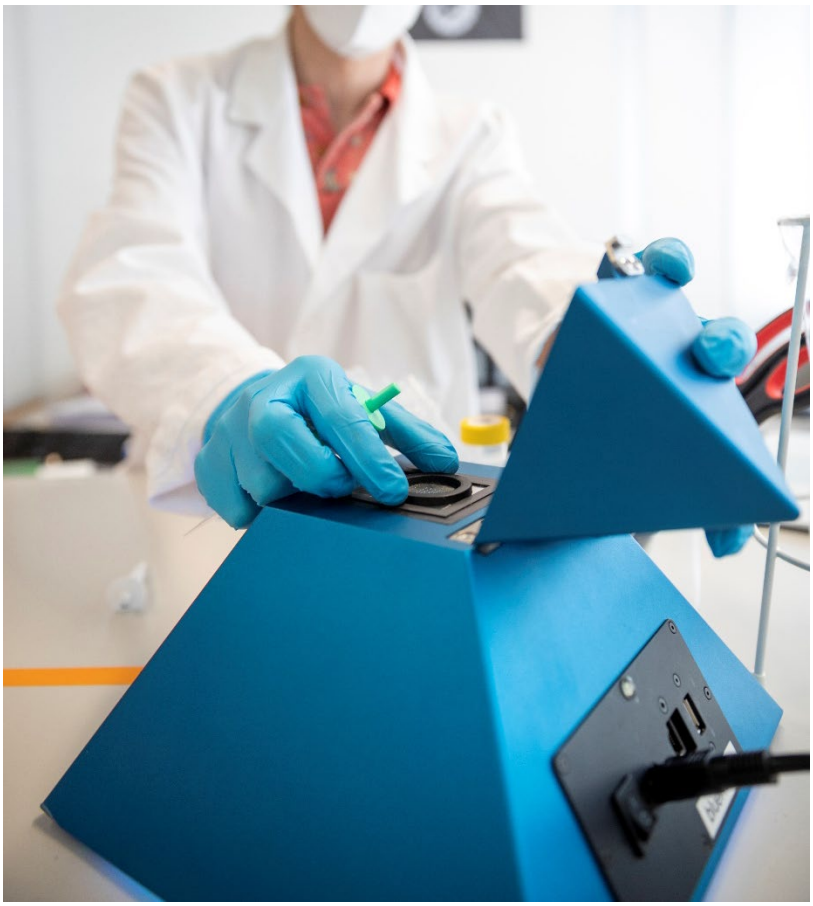

Manuscript submitted:

Philippe Bechtold, Michele Gregorini, Robert N. Grass, Wendelin J. Stark

2.1. Introduction

The COVID-19 pandemic has held a firm grip on the world since its outbreak in December 2019 [74]. In order to limit the spread of the disease, many countries have implemented widespread lockdown rules, that have caused immense economical damage [75]. Widespread scanning of symptoms, such as fever, has been modeled to be ineffective to constrain the spread of the disease [76]. A key strategy to limit infection rates has been the extensive testing of the wide population and subsequent isolation of the infected [77], [78]. A study has shown that random testing is required to contain and control the spread of the disease [79].

Currently, the gold standard for SARS-CoV-2 detection is RT-qPCR from a nasopharyngeal or oropharyngeal swab[80], [81]. The procedure includes the collection of sample from the upper respiratory tract, the extraction of viral RNA from the swab and the amplification of said RNA through RT-qPCR. Several segments of viral RNA are amplified and the amplification is quantified through TaqMan® probes. Advantages of this technique are its high sensitivity and specificity [82], especially when compared to lateral flow RTD's [83]. The major drawbacks of RT-qPCR are however, long reaction times, up to several hours, the high costs of PCR machines and laboratory equipment. Furthermore, sample preparation from the swab is labor- and time-intensive. These constraints lead to the limitation of RT-qPCR to highly specialized and high-throughput laboratories that have been unable to cope with the scope of the ongoing pandemic. Not only were the capacities insufficient until the first wave had passed [84], but the long time to result prolongs the uncertainty period and leads to costs when patients are isolated unnecessarily. As no widespread testing capabilities are available, the barrier for the wide population to get tested regularly is higher.

We have recently developed a qPCR device [72], named peakPCR, which can complete a PCR reaction within less than 20 minutes. An important characteristic of peakPCR is the relatively low cost of each test and the simplicity of usage. The peakPCR device has been shown to perform similar to a state-of-the-art PCR device in terms of efficiency of the reaction and LOD [85]. We have carried out a study with 263 participants to evaluate the possibility of self-testing Sars-CoV-2 using the peakPCR platform. In this publication, we intend to show how engineering of the chip enhances its functionality so that it may be used by non-expert users. The final use of the device may be in small community settings where a healthcare professional is available.

2.1. Materials and Methods

2.1.1. Participants, Setting and Eligibility

Participants were eligible if they were ≥18 years old, mature and able to understand and express themselves well in either English or German.

2.1.2. Recruitment

Participants were recruited through student associations at ETH Zürich and posters on the Hönggerberg campus. Participants who accessed the link for enrollment were screened for eligibility and those eligible were invited.

2.1.3. Assessment of laboratory experience and skills

The participants were divided into 3 cohorts (expert, intermediate, novice) based on their skills with laboratory procedures and their prior laboratory experience (Appendix Table S1).

2.1.4. Preparation of aluminum chips

The RT-qPCR reaction was carried out in an aluminum cartridge with 9 cavities of a volume of 5uL each (see Figure 10). In order to simplify the testing procedure for the user, the cartridges were preloaded with all necessary reagents in a dry form. The mixture of reagents loaded into each well was as indicated in Table 1.

Figure 10. The peakPCR reaction cartridge with gasket and serial number

The layout of the chip was defined as seen in Supplementary Table S2 and Figure 10.

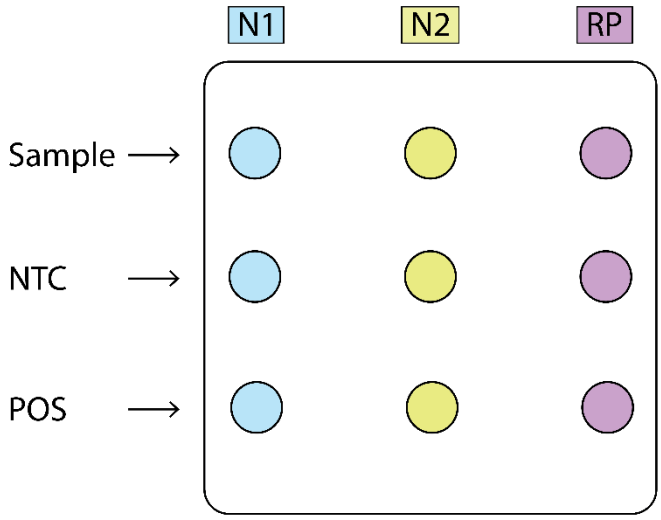

Figure 11. Layout of the chip used in the study. The participants were asked to load their sample in the top row while the bottom two rows were supposed to be filled with RNAse free water. The bottom rows were the no template control (NTC) and the positive control

Table 1. Constitution of the mastermix used for RT-qPCR.

Reagent	Final conc.
Geneon RT-qPCR mastermix	1x
BSA	0.05 µg/uL
MgSO4	1 mM
Forward Primer	500 nM
Reverse Primer	500 nM
TaqMan® Probe	125 nM
Positive control (if used)	5 copies/µL

The chips, preloaded with all necessary reagents, also containing the positive and negative controls as well as cavities for the sample were lyophilized in a Martin Christ Epsilon 2-4 LSCplus. The lyophilisation process consisted of 2 h of cooling down the shelf, on which the chips were loaded, to -55°C, followed by 2 h at -55°C and the pressure being lowered down to 0.1 mbar. The process was kept at these parameters for another 2 h. Then a final drying step was carried out at a pressure of 0.09 mbar and a temperature of the shelf of 25°C. After the lyophilisation process, each chip was individually packed into a vacuum bag containing a drying bag with 2 g of silica.

2.1.5. Procedure of the study

The participants in the study were guided to a working space (Supplementary Figure S1 and Supplementary Figure S2) with all necessary consumables and a laptop displaying instructions via slideshow. All liquids were prefilled into labeled tubes in order to reduce the risk of contamination errors. The first step of the Sars-CoV-2 self-test was the extraction of the sample with a throat swab(Transswab® MW170, MWE) by the participants themselves. The following procedure describes what the optimal method would look be if the participants were to execute each step correctly.

After the swab was taken, it was inserted into a 2 mL Eppendorf tube and 500 µL of a lysis buffer (2 M Guanidinium thiocyanate, 50 mM tris(2-carboxyethyl)phosphine (TCEP), 25 mM sodium citrate, 20 µg/ml of glycogen, pH adjusted to 8-9, in RNase free water (Invitrogen™)) were added with a plastic pasteur pipette. The sample was shaken violently for 30 s and incubated for 5 minutes. The swab was disposed and 400 µL of EtOH (absolute, ≥99.8%, Thermo Fisher Scientific Inc.) were added. Magnetic beads, 10 µL (Turbobeads™) were suspended in the mixture with the help of a 10 µL Minipet (Tricontinent). After mixing by pipetting up and down, the particles were separated by placing the tube into a holder with a magnet (Figure S6). The supernatant was discarded. The tube was removed from the holder and another 400µL of EtOH were added with a plastic Pasteur pipette, whilst making sure the magnetic beads were resuspended well. Separation of the particles was done as before. The final washing step was carried out with 400µL of DMSO. The DNA and RNA were eluted from the magnetic beads through addition of 40µL of RNAse free water with a 40µL Minipet. The resuspended beads were incubated for 3 minutes. The tube was placed into the magnetic holder and 5µL of the supernatant were used to fill each of indicated sample cavities in the aluminum cartridge with the help of a 5µL minipet. The remaining 6 control cavities were filled with 5µL of RNAse free water. The cartridge was covered with approximately 1.5mL of paraffin oil (Scharlau).

Once prepared, the peakPCR cartridge was inserted into the PCR machine [72]. Total runtime of a peakPCR experiment was 37 minutes (Supplementary Table S3).

The remainder of the participant's samples were directly frozen and stored at -20°C until retesting with a reference instrument. Runtime in a Roche Lightcycler 96 was 102 minutes (Supplementary Table S4).

2.1.6. Ethical approval

Approval for this study was obtained from the ETH Ethics commission (ETH-EK-2020-N-52), which also approved of the experimental protocols and questionnaires. All experiments were performed in accordance with relevant guidelines and regulations. All participants signed a form of consent and were informed thoroughly about the study prior to participation.

2.1.7. NPA/PPA

Negative percentage agreement (NPA) and positive percentage agreement (PPA) were determined through comparison of the samples with the Roche Lightcycler 96. If the peakPCR result was inconclusive during the study, it was repeated at a later point with the remainder of the sample that had been frozen. Only samples that were successfully extracted were examined with regards to performance of N1 and N2.

2.2. Results

2.2.1. Participants

263 participants were enrolled to ensure a significant outcome of the study and enable the iteration of the procedure during the study. The exact distribution of age, gender, education and Laboratory skills can be found in Supplementary Table S5. All people participating claimed to not have any symptoms at the moment of participating in the study. The participant flow diagram of the study can be found in Figure 12.

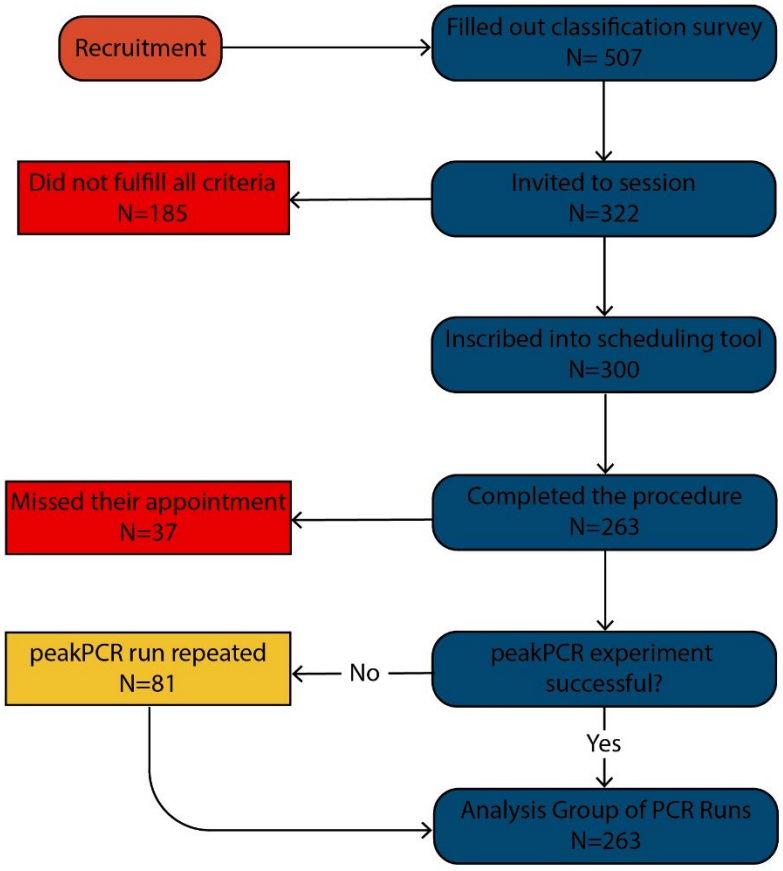

Figure 12. Participant flow diagram of the study. Not all participants scheduled an appointment after being invited and a portion of participants did not show up to the agreed appointment time.

2.2.2. Extraction efficiency and peakPCR success rate

The percentage of successful extractions was determined by testing for the human RNAse P gene with the reference device. Overall, 69.6% were successful, with a higher success rate with people more familiar with laboratory procedures. Of all experiments performed on the peakPCR by

participants, 182 (69.2%) yielded valid results. The success rate of the peakPCR varied as shown in Figure 13.

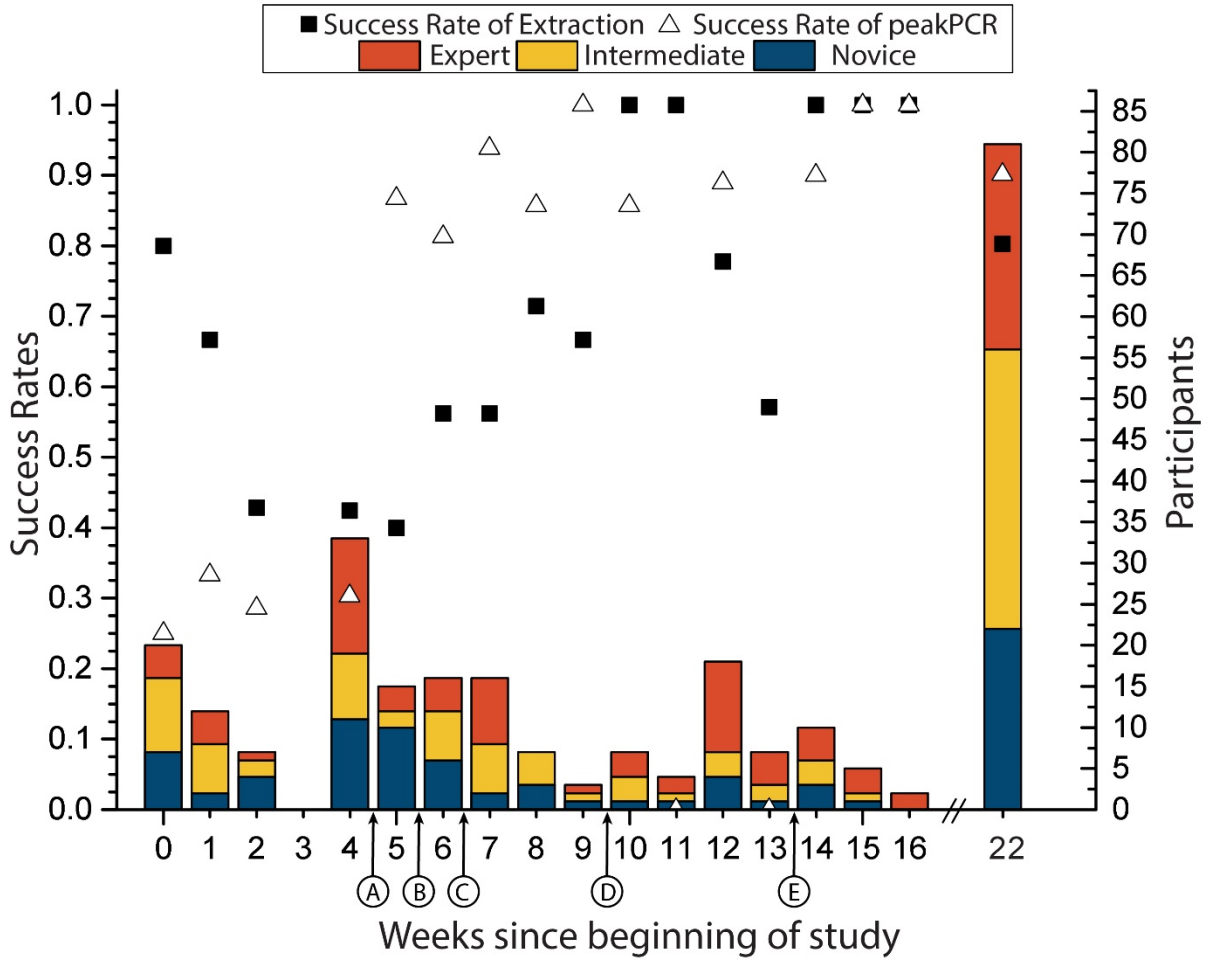

Figure 13. Success rates of extractions and peakPCR respectively as a function of the progression of the study and the number of participants. 5 interventions in the procedure were undertaken. A: The lyophilisation process was changed. The batch size was reduced,

2.2.3. Results of Questionnaire

Participants were handed a questionnaire to give feedback about the quality of the instructions as well as the perceived difficulty of each step. The results can be seen in Table 2

Table 2. Results of questionnaire filled out by participants during the study. The score is given from 1 (lowest/worst) to 10 (highest/best)

Skill level	Expert Score (n)	Intermediate Score (n)	Novice Score (n)	Overall Score (n)
Comprehensibility of swab instructions	8.98 (91)	8.81 (91)	8.97 (78)	8.92 (260)

Easiness of execution of swab	7.43 (90)	7.75 (91)	8.08 (78)	7.74 (259)
Comprehensibility of extraction instructions	8.98 (90)	9.01 (91)	8.97 (77)	8.99 (258)
Easiness of execution of extraction	8.78 (90)	8.57 (90)	8.36 (77)	8.58 (257)
Easiness of particle separation	8.79 (90)	8.72 (89)	8.91 (77)	8.8 (256)
Comprehensibility of PCR instructions	8.91 (89)	8.68 (88)	8.28 (74)	8.65 (251)
Easiness of execution of PCR	8.26 (89)	8 (88)	7.58 (74)	7.97 (251)
Easiness of loading the sample	7.84 (87)	7.52 (87)	6.97 (73)	7.47 (247)
Percentage of people preferring a doctor to perform the test	60.2 (88)	44.9 (89)	56.8 (74)	0.54 (251)

2.2.4. NPA/PPA

All samples were retested for N1, N2 and RP in the reference PCR and the NPA and can be seen in Table 3.

Table 3. Negative and positive percentage agreements of the different PCR reactions run on peakPCR, when compared to a state-of-the art PCR device. For N1 and N2, the resulting PPA 100% (95% CI: 15.8 to 100.0) and NPA 97.8% (95% CI: 94.4 to 99.4) are equal. For the RP gene, the PPA was 98.9% (95% CI: 96.1 to 99.9) and the NPA 96.3% (95% CI: 89.4 to 99.2). As not all of the extractions were successful, the amount of samples tested for N1 and N2 are lower than for RP.

		Reference device								
		N1 +	N1 -	Total	N2 +	N2 -	Total	RP +	RP -	Total
peakPCR	+	2	4	6	2	4	6	181	3	184
	-	0	177	177	0	177	177	2	77	79
	Total	2	181	183	2	181	183	183	80	263

2.3. Discussion

2.3.1. Extraction efficiency

The overall extraction efficiency of the RNAse P gene was 69.6%. Issues with nanoparticles caused drops in extraction efficiencies. This effect was especially visible in weeks 4,5,9 and 13

and the increase in extraction efficiency once the particles were replaced. Once these weeks are excluded, the extraction efficiency rises to 75.6%. The reason for lower efficiencies as the particles were older was the evaporation of the suspension solvent of the stored nanoparticles. In fact, 15 µL of particles were stored in 2mL vials each. The extraction efficiency is higher for participants with high laboratory skills. In fact, 80.6% of highly skilled people managed to produce purified DNA, while 67% of people with intermediate skills were able to complete the procedure with success. For people with no prior laboratory experience, 59.5% were successful. Intervention 2 with the improved instructions helped to clarify the washing steps and gave a significant increase to extraction efficiency (~10%). The third intervention was to give a volume of 200uL of beads to the users instead of 15uL as before. The reasoning behind was that resuspension of magnetic beads is difficult in such small volumes. Together with a new batch of nanoparticles, this intervention increased the success of extraction significantly. Intervention 4 was necessary as the shelf-life of the particles was not sufficient and proved to be highly effective.

2.3.2. Questionnaire

Overall, the instructions were well understood, with the average score throughout all cohorts and experiments being 8.87/10. The lowest scoring instruction were the PCR instructions for novices with 8.26/10. The sampling of the swab was in general the most difficult manual task, surprisingly, highly skilled people found this step more difficult than participants with less skill. Most participants struggled with the gagging reflex and the uncertainty if enough sample was removed. Another difficult task was the loading of the sample into the PCR chip. Skilled participants were more confident in this step than people with no prior experience. A very slight majority of participants would prefer to have a doctor perform the procedure rather than themselves (see Supplementary Figure S2). The overall feedback indicates a lack of trust in their own skills to be the reason. This could be minimized by performing the procedure while a doctor is supervising through a video call or giving direct feedback.

2.3.3. peakPCR success rate

When loading the chip into the peakPCR device and subsequently running the peakPCR, there are multiple potential sources of error. Examples are operator mistakes in loading the sample holder chip, faulty chips or reagents or a malfunctioning of the device. While the overall success rate of the peakPCR experiments was 68.4%, the success rate after Intervention 1 was 83.2% and

if the contaminated batches of chips were excluded, the rate of success was as high as 88.3%. The process of lyophilisation was changed before week 4 of the study. In fact, the batch size was reduced and the transport time to the vacuum packaging machine was reduced. Another change was the prolonging of the lyophilisation program. The prolongation increased the stability of the chips. Unfortunately, the batches used in week 11 and 13 were contaminated with positive control during preparation of the chips. When comparing the different cohorts, the highly experienced participants performed best with 71% managing to get a valid result, 69.2% of intermediate participants received a valid result and 64.6% of novices completed the procedure successfully. As these values are relatively comparable, it can be concluded that most people could perform the procedure, especially if the number of faulty chips was reduced. A more sophisticated quality control protocol could avoid contaminated chips and confirm that the lyophilisation process was successful.

2.3.4. NPA/PPA

As the assay tested for 3 genes individually, 3 NPA and PPA values can be calculated. As the number of positive samples was relatively low (N=2), the PPA of 100% has a 95% confidence interval of 15.8% to 100%. Further experiments with clinical samples will be necessary to increase the meaningfulness of the N1 and N2 tests. However, PPA (98.9%, N=183) and NPA (96.3%, N=80) of the RP Target can be considered as well established. These values indicate a performance of peakPCR that is similar to the state-of-the-art reference PCR device.

2.4. Conclusion

This study has shown that participants were able to perform a complete molecular analysis procedure in most of the cases. Additional support by a remotely monitoring healthcare professional could enhance the portion of successfully completed procedures and the trust of the participants in their results. Together with the peakPCR device, which has shown performances comparable to a state-of-the-art device, the self-testing approach outside of a laboratory becomes conceivable. Further improvements are necessary in the quality control of the test chips. We can therefore conclude that the device can be used in a distributed testing strategy with additional support from a professional. It can be assumed that this help may come either from a telemedicine connection or from a medically educated person in the community where the device is active.

3. Rapid identification of Sars-CoV-2 variants of concern using the portable peakPCR platform

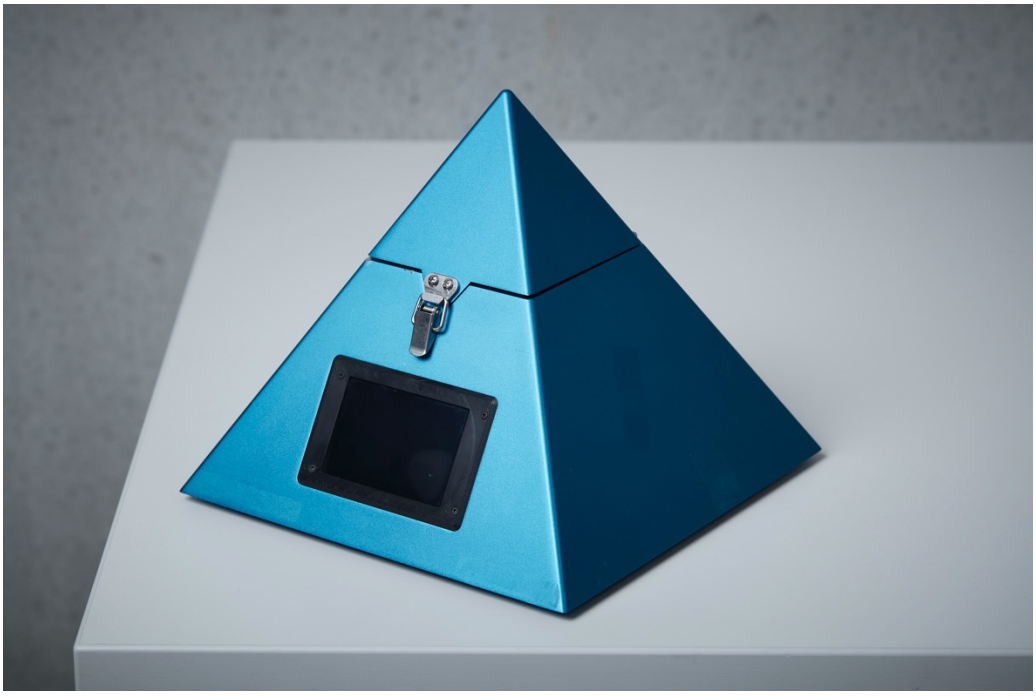

Manuscript accepted as:

Philippe Bechtold, Philipp Wagner, Salome Hosch, Denise Siegrist, Amalia Ruiz-Serrano, Michele Gregorini, Maxmillian Mpina, Florentino Abaga Ondó, Justino Obama, Mitoha Ondo'o Ayekaba, Olivier Engler, Wendelin Stark, Claudia Daubenberger, Tobias Schindler

Analytical Chemistry, ***2021***

3.1. Introduction

More than a year after the World Health Organization (WHO) declared the severe acute respiratory syndrome coronavirus type 2 (Sars-CoV-2) outbreak a Public Health Emergency of International Concern, Coronavirus disease 2019 (COVID-19) has caused more than 3.7 million deaths [86]. Public health systems globally are severely impacted and are further challenged by the emergence of Sars-CoV-2 variants carrying mutations that are of concern (VOC) [87]. Molecular diagnostic tools, particularly reverse transcription quantitative polymerase chain reaction (RT-qPCR) for viral RNA detection and next-generation sequencing (NGS) for molecular monitoring Sars-CoV-2 genetic diversity at the whole genome level have proven critical for public health decision-making [88]. Investigating Sars-CoV-2 genomes by NGS to track transmission chains, understand transmission dynamics and rapidly identify mutations that potentially have an impact on transmissibility, morbidity and mortality as well as potential escape of diagnostic tools or vaccine induced immunity have become an integral part of public health measures during this pandemic [89].

Since the first whole genome sequence (WGS) analysis of Sars-CoV-2 has been published in January 2020 [90], the virus has been continuously sequenced, characterized and data made publicly available through global initiatives such as Global Initiative on Sharing All Influenza Data (GISAID). More than 1.8 million Sars-CoV-2 sequences have been publicly shared via GISAID and numerous mutations in the gene encoding the spike protein have been identified [91]. For example, the D614G variant has been shown to increase the viral load of infected patients and has replaced the original variant since June 2020 around the globe [92]. More recently, Sars-CoV-2 lineages characterized by a combination of multiple mutations in the spike gene have emerged independently in different regions of the world. The Sars-CoV-2 lineages B.1.1.7 (also known as Alpha variant, VOC 202012/01 or 501Y.V1), B.1.351 (also known as Beta variant or 501Y.V2) and P.1 (also known as Gamma variant, B.1.1.28.1 or 501Y.V3) were the first VOCs identified [93]. The Alpha variant (lineage B.1.1.7) was first described in mid-December 2020 in the United Kingdom, the mutation appears to have substantially increased transmissibility and has quickly developed into the dominant variant circulating in the UK and beyond [94]. The Beta variant (lineage B.1.351) was identified in December 2020, emerged most likely in South Africa and is also associated with higher transmissibility [95]. The Gamma variant (lineage P.1) was identified in January 2021 in Manaus, the largest city in the Amazon region of

Brazil [96]. In January 2021, this region experienced an resurgence of COVID-19, despite the reported high seroprevalence of antibodies against Sars-CoV-2 in this population [97],[98]. During the preparation and revision of this manuscript, the WHO had designated the emerging lineage B.1.617.2 as the Delta VOC.

To rapidly detect and continuously monitor the appearance, introduction and spread of (novel) VOCs, the level of molecular surveillance needs to be increased globally. The gold standard of genomic surveillance, NGS, allows unbiased identification of mutations, but is limited by its relatively slow sample-to-result turnaround time and level of laboratory infrastructure and scientific expertise required. Furthermore, the relatively high costs of NGS increase the financial burden on establishing a widespread VOC tracking strategy, a limiting factor particularly for resource-limited settings. Therefore, mutation-specific PCR-based approaches which are more cost-efficient and allow for high-throughput screening of a significant proportion of Sars-CoV-2 positive individuals were developed [99], [100]. To identify transmission dynamics of VOCs in settings with limited sequencing capabilities, we have designed rapid and cost-effective RT-qPCR assays detecting relevant mutations in the spike protein of Sars-CoV-2. The N501Y mutation is found in Alpha, Beta and Gamma VOCs, while the E484K mutation is restricted to Beta and Gamma variants. The Alpha variant is characterized by an additional spike gene deletion (ΔHV69/70). To further simplify, decentralize and speed up the process of VOC identification, we transformed our assay to a portable and inexpensive qPCR device, named peakPCR [72]. The device can complete up to 20 RT-qPCR reactions in less than 40 minutes. Important characteristic of peakPCR are the relatively low cost of production and the simplicity of usage. By using cartridges that are preloaded with lyophilized RT-qPCR reagents, the user interaction is reduced to loading the sample onto the cartridge. Furthermore, the preloaded peakPCR cartridges can easily be shipped and stored at room temperature, making cold chains superfluous. Here, we report the development of a new approach for rapid, robust and decentralized identification of Sars-CoV-2 VOC which can be both run on standard laboratory RT-qPCR equipment and the portable and rapid diagnostic technology platform peakPCR.

3.2. Material and Methods

3.2.1. Sars-CoV-2 cell culture supernatants and clinical samples for assay evaluation

The cultivation of SARS-CoV-2 was carried out in a Biosafety level 3 laboratory and conducted under appropriate safety conditions. Three different VOC lineages of Sars-CoV-2, namely B.1.1.7, B.1.351 and P.1 provided from University Hospital of Geneva, Laboratory of Virology were grown on VeroE6/TMPRSS2 cells obtained from the Centre For AIDS Reagents (National Institute for Biological Standards and Control) [101], [102]. The day before infection VeroE6/TMPRSS2 cells were seeded at 2x106 cells per T75 flask in DMEM (Seraglob, Switzerland) supplemented with 10% FBS (Merck, Germany) and 2% SEeticin (Seraglob, Switzerland). At the day of infection, the cells reached about 70-90% confluency. The growth medium was removed and replaced with 5 mL of infection medium (DMEM+2% FBS+2% SEeticin). Cells were inoculated with 70 µL of SARS-CoV-2 swab material and incubated for 1 h at 37°C, 5% CO2, and >85% humidity. After the adsorption, 10 mL of infection medium was added to each flask. Cells were observed for cytopathic effects (CPE) for 3-6 days using EVOSTM FL Digital Inverted Microscope. When CPE reached 40-100% the supernatant was collected, cleared from cell debris by centrifugation (10 min at 500g) and samples were aliquoted and frozen. TCID50 was determined on VeroE6/TMPRSS2 cells. Virus was inactivated with Qiazol and RNA was extracted with RNeasy Plus Universal Mini Kit (Qiagen, Germany).

As a positive control and for initial assay evaluation a 1869 bp long synthetic Sars-CoV-2 spike gene fragment (genome position 21,557-23,434 bp), based on the sequence of B.1.1.7 was synthesized (Sequence is provided as Figure S1). Using a serial dilution of the synthetic spike gene a calibration curve ranging from 0.05 to 50,000,000 copies/µL was prepared (data provided in as Figure S2). The initial viral copy number per µL (cp/µL) of the cell culture derived RNA from Sars-CoV-2 was estimated using the calibration curve's y-intercept and its slope. Serial dilutions of the RNA extracted from culture supernatants of Sars-CoV-2 isolates Wuhan Hu-1, B.1.1.7, B.1.351 and P.1, ranging from 0.1 to 1,000,000 cp/µL was prepared and used to evaluate the assays' performance on both RT-qPCR platforms. Additionally, a Sars-CoV-2 RT-qPCR diagnostic assay, targeting the envelope (E) gene, published by the Institute of Virology at Charité (Berlin, Germany), was used as a positive control for viral RNA on both platforms [103].

3.2.2. Designing HV69/70-deletion-, E484K- and N501Y-specific RT-qPCR assays

We developed assays targeting the HV69/70-deletion, the E484K-, and N501Y-single nucleotide polymorphisms (SNP). For standard RT-qPCR platforms like the Bio-Rad CFX96 device, multiplex assays were developed. The multiplex assays are able to detect both sequence variations, the wildtype and mutated, in a single RT-qPCR reaction. For rapid identification of mutations of interest for mobile and rapid RT-qPCR platforms, such as the peakPCR device, only the mutated sequence variation is detected and no multiplex amplification is performed. SNP discrimination was enhanced by using primers and probe containing Locked Nucleic Acids (LNAs). Sequence analysis and primer design were done using the Geneious Prime® 2021.0.3 software. All oligos, including the LNAs, were synthesized at Microsynth AG (Balgach, Switzerland) and details are provided in Table 4.

3.2.3. Sars-CoV-2 HV69/70-, E484K- and N501Y-specific RT-qPCR assays

The HV69/70-, E484K- and N501Y-specific assays were performed using the Bio-Rad CFX96 Real-Time PCR System (Bio-Rad Laboratories, California, USA). A RT-qPCR run was completed within 1 hour and 10 min using the following thermal profile: reverse transcription step at 50 °C for 5 min; polymerase activation 95 °C for 20 s; and 45 cycles of 3 s at 95 °C and 30 s at 61 °C. Each reaction consisted of 2 µL RNA and 8 µL reaction master mix containing 1x TaqMan™ Fast Virus 1-Step Master Mix (Thermo Fisher Scientific, Leiden, The Netherlands) and the corresponding 1x primer/probe mixture consisting of 0.4 µM primers and 0.2 µM probes. All RT-qPCR assays were run in duplicates with appropriate controls. The mutated sequences were detected by FAM-labelled probes and the wildtype sequences by Yakima-Yellow-labelled probes in multiplex reactions. Data analysis of the RT-qPCR data was conducted using CFX Maestro Software (Bio-Rad Laboratories, California, USA). RT-qPCR amplification efficiencies were calculated based on the slope of the standard curve as described elsewhere [104].

The HV69/70-, E484K- and N501Y-specific RT-qPCR assays were transferred to the peakPCR platform (Diaxxo AG, Zurich, Switzerland) on which FAM-labelled probes detected the mutated sequence variations only. In order to simplify the testing procedure for the user, the peakPCR aluminium sample holders (herein referred to as cartridges) were preloaded with all necessary reagents in a freeze-dried form. Lyophilized cartridges were loaded with 4.4 µL sample, sealed off with 1.2 mL of paraffin oil (Sigma–Aldrich, Germany) and run on the peakPCR device using the following program: reverse transcription step at 50 °C for 5 min; initial denaturation at 95 °C

for 60 s; and 45 cycles of 6 s at 95 °C and 30 s at 62 °C. Total runtime of a peakPCR experiment was 37 minutes. PeakPCR data was analysed using the peakPCR dataAnalysis 1.0 software (Diaxxo AG, Zurich, Switzerland). No drop in performance was observed when lyophilized reagents were used compared to non-lyophilized standard RT-qPCR reagents (Figure S3).

3.2.4. Evaluation of diagnostic performance with clinical samples

Clinical evaluation was conducted using RNA extracted from Sars-CoV-2 positive samples collected in Equatorial Guinea. Sample collection and analysis was done as part of a research collaboration with the Equato-Guinean Ministry of Health and Social Welfare and was enabled by several presidential emergency decrees. All patient data were fully anonymized and publication was approved by the National Technical Committee for the Response and Monitoring of the Novel Coronavirus (Comité Técnico Nacional de Respuesta y Vigilancia del Nuevo Coronavirus), which is charged with preventing, containing, controlling, tracking and evaluating the development and evolution of COVID-19 in Equatorial Guinea.

3.2.5. MinION Sars-CoV-2 whole genome sequencing

A total of 59 Sars-CoV-2 positive samples from Equatorial Guinea were selected for reconfirmation using whole genome sequencing (WGS) by MinION (Oxford Nanopore Technologies, Oxford, UK) according to the open-source ARTIC protocol (https://artic.network/ncov-2019). Sample preparation for MinION sequencing was based on the ARTIC Network nCoV-2019 sequencing protocol v2 [105] and v3 [106]. The RNA samples were diluted in nuclease-free water according to their cycle threshold value in the diagnostic RT-qPCR. (Cq <15: 1:100 dilution, Cq 15-18: 1:10 dilution) for cDNA synthesis, for which either SuperScript IV Reverse Transcriptase (Thermo Fisher Scientific, USA) or LunaScript™ RT SuperMix (New England BioLabs, USA) was used with random hexamer primers. A total of 218 primer pairs covering the whole virus genome were used for PCR amplification [107]. The ligation sequencing kit (Oxford Nanopore Technologies, UK) was used for library preparation. Sequencing was conducted on a FLO-MIN106 (R9.4.1) flow cell. Base calling was performed in real time on a MinION Mk1c using MinKNOW version 20.10.6. The ARTIC Network bioinformatics protocol was followed for data analysis [108]. Consensus sequences were generated with Wuhan-Hu-1 isolate (GenBank accession number MN908947.3) as a reference sequence. Variants were called using Nanopolish and Medaka. Lineage assignment was done using the pangolin tool [109]. All sequences were deposited to GISAID.

3.3. Results

3.3.1. Design of RT-qPCR assays for rapid identification of Sars-CoV-2 VOCs

Three mutation-specific RT-qPCR assays based on TaqMan® chemistry were designed. The first assay targets the 6 bp deletion in the spike gene leading to the loss of two amino acids at positions 69 and 70 within the spike protein (HV69/70 assay). This deletion is found in the Alpha VOC, but not in Beta or Gamma VOCs. Universal primers amplify a 102-bp (wildtype) or 96-bp (mutant) amplicon. Based on the presence or absence of the deletion, either a FAM-labelled probe or YYE-labelled probe binds and the resulting fluorescence is detected. The second assay targets a non-synonymous SNP in the spike gene (A23011G) leading to an amino acid exchange at positions 484 (E484K). The E484K mutation is only present in Beta and Gamma VOCs. In a multiplex reaction, a YYE-labelled probe detects the wildtype and a FAM-labelled probe the mutated sequence. The third assay targets a non-synonymous SNP in the spike gene (A23063T) leading to an amino acid exchange at positions 501 (N501Y). The N501Y mutation is present in Alpha, Beta and Gamma VOCs. Similar to the E484K assay, a YYE-labelled probe detects the wildtype and a FAM-labelled probe the mutated sequence. A summary of the oligonucleotide sequences used are provided in Table 4. Wildtype sequences are defined as the nucleotide sequences of the original Wuhan Hu-1 isolate published [110].

Table 4. Primer and probe combinations developed for Sars-CoV-2 VOC identification and discrimination.

Assay	Primer name	Oligo sequence (5'-3')	Modifications
HV69/70 assay:	HV69/70_F	TCA ACT CAG GAC TTG TTC TTA CCT	
21765-21770*	HV69/70_R	TGG TAG GAC AGG GTT ATC AAA C	
deletion in Alpha	HV69/70 (wt)	ACA TGT CTC TGG GAC CAA TGG	YYE† - BHQ1
VOC	Δ69/70 (mut)	TCC ATG CTA TCT CTG GGA CCA	FAM - BHQ1
N501Y assay:	spike_gene_ LNA_F	C+TA TCA GGC +CGG TAG CAC +AC	
A23063T* SNP in	spike_gene_ LNA_R	+AGT ACT ACT ACT CTG TAT +GGT TGG +T	
Alpha, Beta and	501Y_LNA (mut)	C+CC A+CT +**t**+AT G+GT +G	FAM - BHQ1
Gamma VOCs	N501_LNA (wt)	C+CC A+CT +A+AT G+GT +G	YYE† - BHQ1
E484K assay:	Spike_gene_ LNA_F	C+TA TCA GGC +CGG TAG CAC +AC	
G23011A* SNP in	Spike_gene_ LNA_R	+AGT ACT ACT ACT CTG TAT +GGT TGG +T	
Beta and Gamma	484K_LNA (mut)	TGG +T+GT T**a**A A+GG T	FAM - BHQ1
VOCs	E484_LNA (wt)	TGG +T+GT TGA A+GG T	YYE† - BHQ1

* Genome position according to MN908947.3 (Sars-CoV-2 isolate Wuhan-Hu-1). LNA nucleotides are indicated with + in front of the nucleotide. The SNP associated with VOCs is indicated as lower case and bold nucleotides. † YYE=Yakima Yellow (VIC & HEX dye alternative)

The novel assays were run on two different RT-qPCR platforms in parallel. On the Bio-Rad CFX96 platform (Figure 14A), the three sequence-discriminatory assays were run as duplex assays, detecting the wildtype sequence in the YYE channel (Figure 14B) and the mutated sequence in the FAM channel (Figure 14C). As a second technology platform the peakPCR device was selected (Figure 14D), which is a portable and rapid diagnostic technology platform running the RT-qPCR reaction on ready-to-use cartridges (Figure 14E). Fluorescence is detected using the Raspberry Pi Camera Module V2 as an inexpensive CCD sensor (Figure 14F). For the peakPCR device the multiplex assays were reduced to mutation-specific assays, capable of detecting the mutated sequences only.

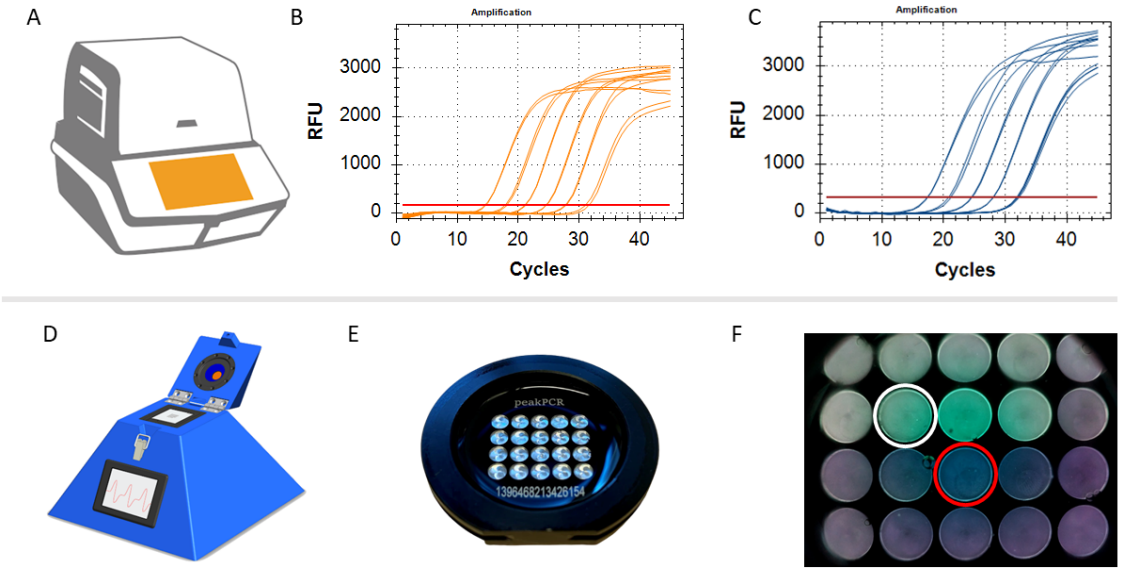

Figure 14. RT-qPCR platforms for Sars-CoV-2 VOC identification. A) Standard RT-qPCR device Bio-Rad CFX96. B) Detection of N501Y-wt in serial dilution of Wuhan Hu-1 lineage, ranging from 1-10'000 cp/µL using the YYE-channel of the Bio-Rad CFX96 instrument. C) Detection of N501Y-mut in serial dilution of P.1 lineage, ranging from 1-1'000'000 cp/µL using the FAM-channel of the Bio-Rad CFX96 instrument. D) Portable and rapid diagnostic platform peakPCR. E) Ready-to-use cartridges with preloaded lyophilized RT-qPCR reagents. F) Photo after cycle 45 detecting fluorescence in each well with an CCD sensor. The depicted well marked with a white circle contains a positive signal after RT-qPCR amplification, while the negative sample, marked with a red circle, did not display an amplification of a PCR product.

3.3.2. Analytical performance of HV69/70, E484K, and N501Y assays using well-characterized RNA from Sars-CoV-2 VOCs

Four Sars-CoV-2 lineages, namely Wuhan-Hu-1 (wildtype), B.1.1.7 (Alpha), B.1.351 (Beta) and P.1 (Gamma), were used to assess the RT-qPCR efficiency, specificity and sensitivity of the novel mutation-specific assays. We used serial dilutions, ranging from 1 to 1,000,000 cp/µL, of cell culture derived viral RNA for assay characterization. The presence and quantity of RNA molecules in these serial dilutions was confirmed by monitoring the pan-Sarbecovirus E-gene amplification (Figure 15A). Mutation-specific assays for the HV69/70 (Figure 15B), E484K (Figure 15C), and N501Y (Figure 15D) were run on both platforms, while wildtype-specific assays were solely run on the Bio-Rad CFX96 platform. The data provided in Figure 15 was used to obtain RT-qPCR amplification efficiencies, sensitivities and specificities shown in Figure 16.

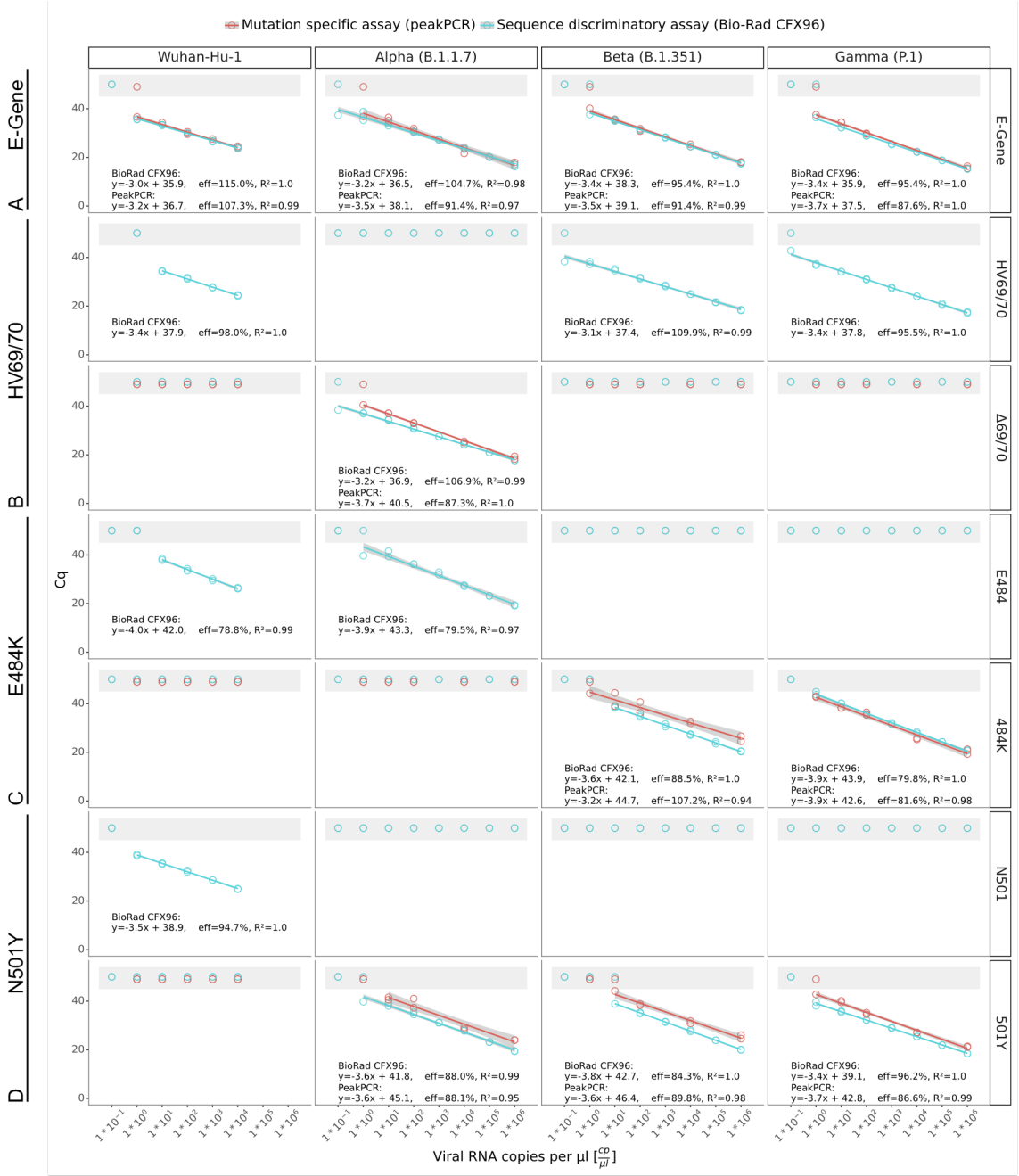

Figure 15. RT-qPCR performance of novel Sars-CoV-2 mutation-specific assays. A) Sars-CoV-2 E-gene reference assay C) HV69/70 assay, C) E484K assay and D) N501Y assay. Each circle represents a technical replicate. Mutation-specific assays were run on both platforms, while wildtype-specific assays were only run on the Bio-Rad CFX96 platform. For the Wuhan-Hu-1 lineage, the two highest RNA concentrations of 1,000,000 and 100,000 cp/µL were not available. Tests for performance on the peakPCR device used the 1,000,000 cp/µL, 10,000 cp/µL, 100 cp/µL, 10 cp/µL, and the 1 cp/µL concentrations. The Cq values for samples without amplification are set arbitrarily to 46 for the peakPCR and 47 for Bio-Rad CFX96 devices. Data points within the grey area are considered negative (Cq values > 45).

RT-qPCR amplification efficiencies for all assays were calculated (Figure 16A). High amplification efficiencies (> 90%) were obtained for the E-gene, the HV69/70 and E484K assays on the Bio-Rad CFX96 platform and for the E-gene and E484K assays on the peakPCR device. All other assays achieved amplification efficiencies > 80% which is considered moderate. The analytical sensitivity of the assays was defined as the lowest viral RNA concentration at which mutations are identified in >80% of replicates. We used the detection rate among all replicates combined for all four Sars-CoV-2 lineages to identify the Limit of Detection (LOD) (Figure 16B). For the E-gene, HV69/70, and E484K assay a detection rate of 100% was achieved at viral RNA concentration as low as 10 cp/µL. At the same concentration for the N501Y assay, 5 out of 6 replicates (83%) were amplified. At the LOD of 10 cp/µL (dashed line in Figure 16B) no difference between the two RT-qPCR platforms in terms of sensitivity was observed. Viral RNA concentrations below 10 cp/µL cannot be detected, with exception of the HV69/70 assay run on the Bio-Rad CFX96 device, where 1 cp/µL is still reliably detected.

Specificity of all three assays and their ability to distinguish between mutated and wildtype sequences were assessed by testing the assays with RNA from Sars-CoV-2 cell culture supernatants. On both platforms, no signal was observed at any viral RNA concentration if there was not a perfect sequence match of the oligos to the nucleotide sequence to be detected, resulting in a 100% analytical specificity. At a viral RNA concentration of 10'000 cp/µL, the HV69/70, E484K, and N501Y genotypes were all correctly identified (Figure 16C). The mutation-specific probe of the HV69/70 assay gave a signal only when run with RNA of the B.1.1.7 lineage carrying the mutation. The E484K-mutation assay did not result in amplification when run on RNA from Wuhan Hu-1 and B.1.1.7 lineage. The N501Y-mutation assay detected correctly all VOCs but not the Wuhan Hu-1 lineage. In summary, the three assays correctly identify lineage-associated mutations with moderate to high RT-qPCR efficiencies in samples with more than 10 cp/µL of Sars-CoV-2 RNA. We also demonstrated that these assays can be successfully conducted on the rapid diagnostic platform peakPCR and the performance in terms of sensitivity and specificity does not significantly differ between these two RT-qPCR platforms.

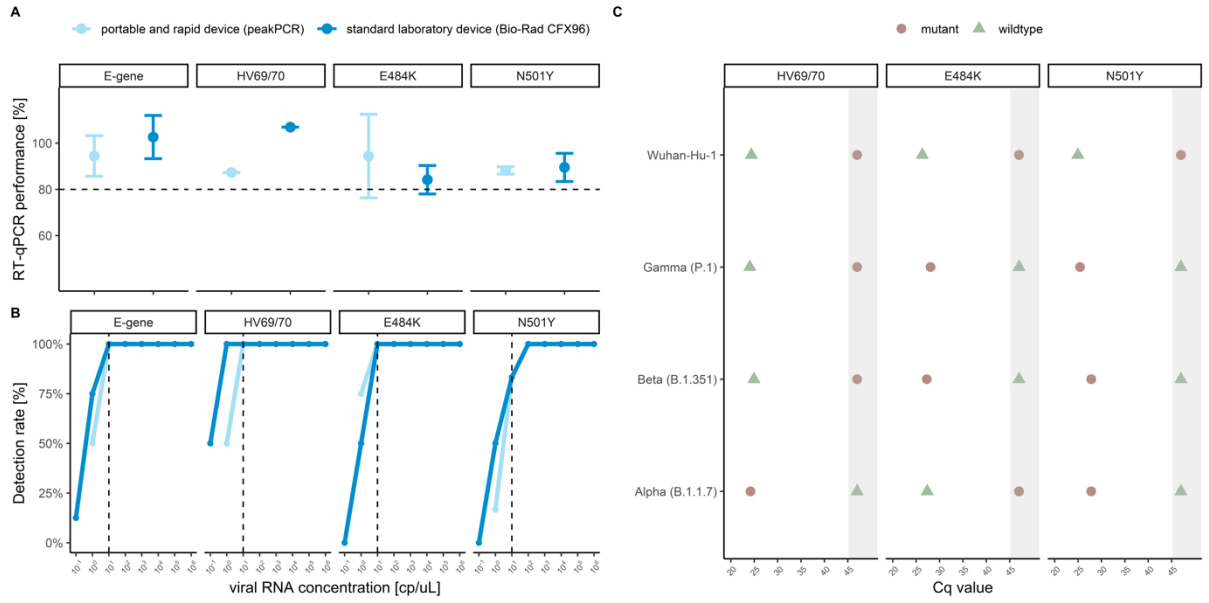

Figure 16. Analytical performance of HV69/70, E484K, and N501Y detecting RT-qPCR assays. A) RT-qPCR amplification efficiency of the E-gene, HV69/70, E484K and N501Y assays as determined by serial dilutions of RNA derived from four cell culture supernatant Sars-CoV-2 lineages. Amplification efficiencies > 80% are considered moderate (dashed lines). B) Analytical sensitivity represented by detection rates calculated from all replicates for each viral RNA concentration. The Limit of Detection (LOD) was defined as the lowest concentration at which >80% of replicates were amplified. The dashed line represents the LOD of 10 copies per µL. C) Analytical specificity for the multiplex sequence-discrimination assays run on the Bio-Rad CFX96 device. The data shown are based on RT-qPCR amplification for viral RNA concentrations of 10'000 cp/µL. Data points within the grey area are considered negative (Cq values > 45).

3.3.3. Clinical performance of HV69/70, E484K, and N501Y detecting RT-qPCR assays

We used 59 clinical samples positive for Sars-CoV-2 collected in Equatorial Guinea between November 2020 and March 2021 for further evaluation of all three mutation-specific RT-qPCR assays. The outcome of the RT-qPCR assays were compared to Nanopore MinION-based Sars-CoV-2 whole genome sequencing data obtained from the same clinical samples (Table 5). The HV69/70 assay identified the spike gene deletion Δ69/70 correctly in 2 out of 2 samples, while for all other samples, in accordance with WGS, the wildtype HV69/70 genotype was found. The E484K assay accurately identified the 484K SNP in 43 samples with the Beta VOC and in one sample assigned to the B.1.620 lineage. The N501Y assay genotyped all 59 samples correctly allowing the identification of one Alpha and 43 Beta VOCs. In summary, the evaluation with clinical samples resulted in a 100% agreement between the novel mutation-specific RT-qPCR assays and Sars-CoV-2 WGS.

Table 5. Performance evaluation of HV69/70, E484K, and N501Y detecting RT-qPCR assays using clinical samples.

Sars-CoV-2 lineage	Mutation profile**	n	HV69/70	Δ69/70	E484	484K	N501	501Y
Wild type*	HV69/70, E484, N501	14	14/14	0/14	14/14	0/14	14/14	0/14
Alpha (B.1.1.7)	Δ69/70, E484, 501Y	1	0/1	1/1	1/1	0/1	0/1	1/1
Beta (B.1.351)	HV69/70, 484K, 501Y	43	43/43	0/43	0/43	43/43	0/43	43/43
B.1.620	Δ69/70, 484K, N501	1	0/1	1/1	0/1	1/1	0/1	0/1

*includes the following Sars-CoV-2 lineages: B.1, B.1.1, B.1.177, B.1.192, B.1.36.10, B.1.535, B.1.596, B.1.623

**based on Sars-CoV-2 whole genome sequencing

3.3.4. Investigating the introduction and spread of Sars-CoV-2 Beta VOC in Equatorial Guinea using mutation-specific RT-qPCR assays

In total we analysed 184 Sars-CoV-2 positive samples from Equatorial Guinea using all three mutation-specific RT-qPCR assays collected from November 2020 to March 2021 (Figure 17A). While between November and December 2020, all samples were wildtype for the three spike gene mutations associated with Sars-CoV-2 VOCs, starting from January 2021, more than 85% (102/119) of samples carried the 484K+501Y mutant combination. WGS analysis of a subset of these samples revealed an expansion of the Sars-CoV-2 Beta VOC (lineage B.1.351) in Equatorial Guinea (Figure 17B). Other combinations of mutations of interest were also found, the sample with Δ69/70+501Y was identified as the Alpha variant (B.1.1.7 lineage) and the sample with Δ69/70+484K was identified as the B.1.620 lineage. In summary, these RT-qPCR-based assays enable rapid and cost-effective genotyping of larger numbers of clinical samples resulting in a more accurate reflection of Sars-CoV-2 epidemiology and their local transmission dynamics.

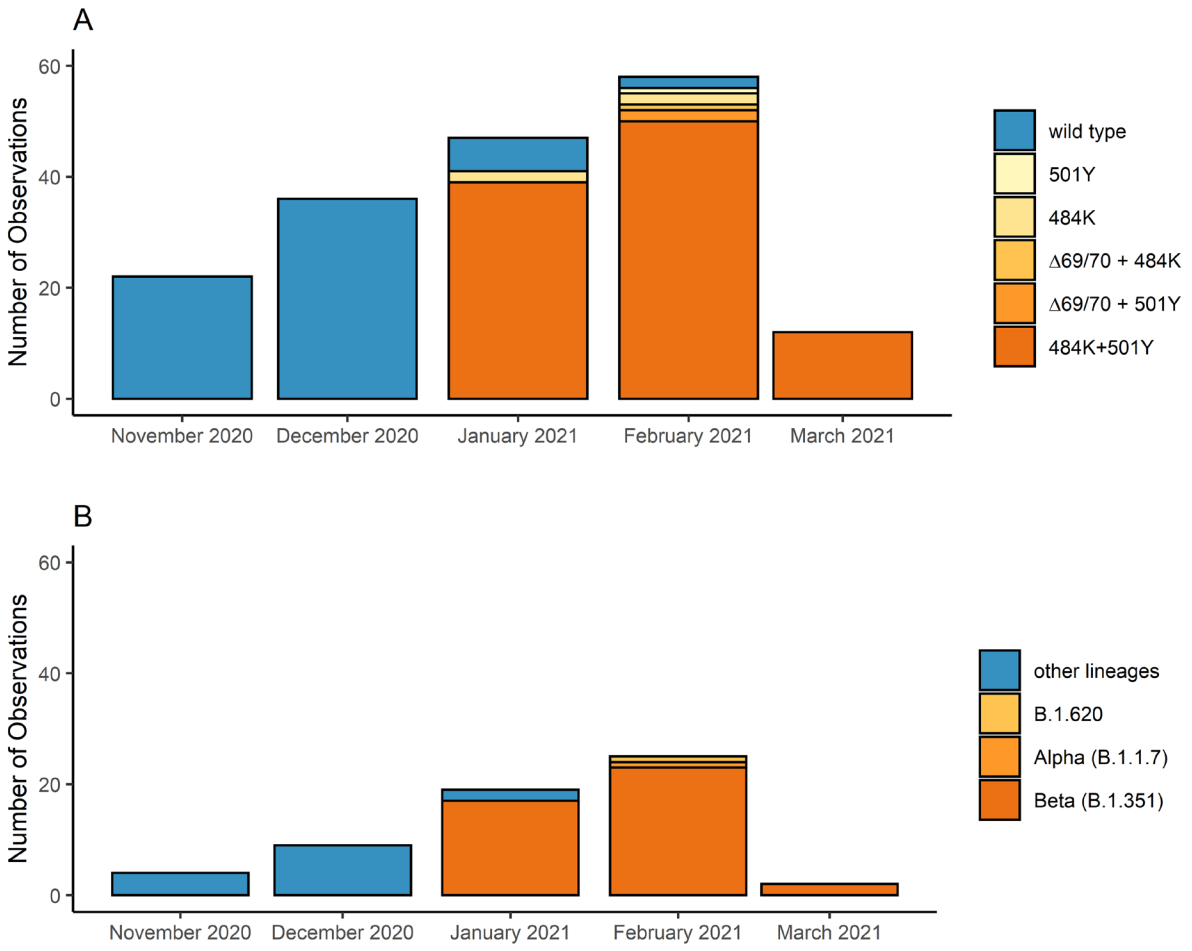

Figure 17. Rapid detection of Sars-CoV-2 VOC-associated mutations using HV69/70, E484K, and N501Y RT-qPCR assays. A) Identification of spike gene mutations using HV69/70, E484K and N501Y RT-qPCR assays in 184 clinical samples collected in Equatorial Guinea from November 2020 to March 2021. B) Identification of Sars-CoV-2 lineages using Nanopore MinION Sars-CoV-2 whole genome sequencing in 59 clinical samples collected in Equatorial Guinea from November 2020 to March 2021.

3.4. Discussion

The COVID-19 pandemic is a continuous, unprecedented, global public health crisis with severe economic and social consequences [111]. More than one year into the pandemic, the emergence of VOCs starts to pose again serious threat to contain the virus. Rapid and reliable identification of SARS-CoV-2 variants is a critical component of public health interventions to mitigate the further spread of VOCs that might undermine performance of diagnostic tests and vaccine induced immunity against this virus [112].

We designed, tested and validated three mutation-specific RT-qPCR assays, detecting the E484K and N501Y SNPs as well as the 6-bp deletion affecting HV69/70, all located in the Sars-CoV-2

spike gene. All assays can be performed under standard RT-qPCR conditions simplifying integration into existing laboratory environments and proved to be highly sensitive, specific, and reproducible. We demonstrated the usefulness of such screening assays to rapidly identify potential VOCs using clinical samples. Using our assays we were able to observe the introduction and spread of the B.1.351 lineage in Equatorial Guinea. Its noteworthy that it took less than four weeks for the B.1.351 lineage to become the dominant lineage in this cohort. Using more than one VOC marker enabled us to identify Sars-CoV-2 variants with an unusual combinations of mutations, such as the E484K plus the HV69/70 deletion. This sample was later assigned to the Sars-CoV-2 lineage B.1.620 which is most likely of Central African origin and has recently been described in several countries in Europe [113].

The approach presented here is well-suited for cost-effective, robust and high-throughput screening of large cohorts. Mutation-specific RT-qPCRs are not intended to replace NGS, but rather complement and extend molecular surveillance programs and focal outbreak monitoring. During the preparation of this manuscript, the WHO had designated the lineage B.1.617.2 as the fourth VOC. The Delta variant (lineage B.1.617.2) was first documented in India, where it has contributed to the surge in cases and has now been detected across the globe [114]. Based on the perfect mismatch discrimination of LNA-based assays and the simplicity of this type of assay in both, design and implementation, will allow rapid adaptation of our approach to B.1.617.2 and also to newly emerging VOCs identified in future.

A similar LNA-based approach for detection of N501Y and HV69/70 has been successfully tested in Canada on 2,430 samples [115]. The results of their in-house assay were concordant with the commercial assay VirSNiP SARS-CoV-2 (TIB Molbiol, Berlin, Germany) which is based on melting-curve analysis. This underlines the possibility of using LNA-based RT-qPCR assays for single-nucleotide discrimination as opposed to using melting-curve analysis. Although the Sars-CoV-2 SNP genotyping by melting-curve analysis is widely used [116], the LNA-based approach has several advantages: It is faster, easier to integrate into existing laboratory workflows and could be combined with a diagnostic assay allowing immediate genotyping. Furthermore, LNA-based sequence-discriminatory assays are better suited to identify presence of more than one lineage of SARS-CoV-2 in a single sample, a phenomenon which was recently observed in Brazil [117].

To reduce the sample-to-result turnaround time in routine, decentralized testing settings, our strategy included the transfer of these assays to a portable, robust and rapid diagnostic RT-qPCR

platform. Starting from extracted RNA, the peakPCR platform completed sample analysis in 37 minutes, which is half of the time required to run the same assay on a standard RT-qPCR platform while retaining comparable efficiency, specificity and sensitivity. For the first time, we show that complex RT-qPCR based genotyping assays can be transferred to the rapid and portable peakPCR platform. Apart from the speed, and the simplicity of usage, the relatively low costs of equipment and reagents make this platform interesting. The peakPCR device costs are an estimated $2500, a fraction of the price at which commercially available qPCR devices are being sold and due to the lower reaction volume used in peakPCR experiments (4 µL), the costs per pre-loaded and freeze-dried 20-well cartridge is kept similar to the reagent costs for a standard RT-qPCR reaction.

3.5. Outlook

Future technological developments will focus on simplified sample pre-processing strategies to replace the RNA extraction step completely. This would allow placement of this molecular diagnostic platform in non-laboratory settings. Furthermore, deployment of cartridges preloaded with lyophilized reagents independent from cold chain for reagent supply are significant technological advantages which make this platform well-suited for decentralized, rapid molecular testing of infectious diseases, particularly in resource limited settings.

4. Highly sensitive malaria parasite detection within 30-minutes: peakPCR as a point-of-care solution

Manuscript submitted:

Philippe Bechtold, Philipp Wagner, Salome Hosch, Wendelin J. Stark, Claudia A. Daubenberger,

Tobias Schindler and Ulrich Vickos

4.1. Introduction

Malaria is an infectious disease caused by different Plasmodium spp. species and is trans-mitted through the female Anopheles spp. mosquitoes [118]. Although significant progress on combating the spread of the disease, more than 400’000 people still die annually [119]. In order to reach the WHO goal of 2030 to eliminate of malaria and to reduce the number of serious courses of the disease, vast improvements in the accuracy and availability of diagnostics need to be made [120]. Currently employed methods comprise blood smear microscopy, antigen rapid diagnostic tests (RDT) and nucleic acid amplification tests (NAAT) [121]. Diagnosis of malaria by observation of Giemsa-stained thick or thin blood smears has been the gold standard for a long time. Well trained and experienced microscopists can reach limit of de-tection (LOD) of 50-100 parasites/µL [122]. Expert microscopists are however chronically lacking and the sample throughput is rather low. RDT’s are low-cost and widely available with 460 million tests distributed and sold annually [119]. RDTs are based on detection of parasite antigens and can provide valuable and rapid answers in remote areas without the need for extensive training. However, their high LOD, which is 100-200 parasites/µL for PfHRP2-based RDTs [123] and about 1000 parasites/µL for panLDH-based RDTs [124] and subsequently low sensitivity makes them unsuitable in endemic and low-transmission environments [125]. NAAT’s such as polymerase chain reaction (PCR) have shown extremely low LOD’s of 0.05 parasites/uL [126], which may be useful to detect asymptomatic carriers of the disease. This ap-proach is especially needed in areas where malaria is almost eradicated [127]. The use of highly sensitive PCR testing has been restricted to large centralized laboratories which are inacces-sible for most of the population because of cost and the need for trained personnel [128].

The peakPCR platform has already been shown to deliver results similar to a state-of-the-art PCR device[85]. In this publication, we investigate peakPCR for its use as a rapid and highly sensitive NAAT-based diagnostic tool for malaria and compare it to other currently availa-ble diagnostic tests.

4.2. Material and Methods

4.2.1. Study population and collection of clinical samples

The study was conducted at the Paediatric Hospital and University Complex of Bangui (CHUPB), located in the Central African Republic (CAR). The patients were children aged between 5 months and 15 years that were admitted to the emergency department with fever as their main symptom. During March 8th to March 13th 2021, a total of 100 children were recruited into the study. Whole blood samples were collected in EDTA blood collection tubes. Malaria RDTs (CareStart™ Malaria HRP-2/pLDH Pf/Pan Combo Test), thick blood smear (TBS) microscopy and a complete blood count were routinely performed. An aliquot of the whole blood was prepared as dried blood spots (DBS) on filter paper. The DBS were stored at room temperature and sent to the Swiss Tropical and Public Health Institute, Basel, Switzerland for molecular analysis. The study protocol was approved by the Scientific Committee of the Faculty of Health Sciences of the University of Bangui, CAR and supported by the national malaria control program of the CAR.

4.2.2. Molecular analysis of malaria parasites using nucleic acids extracted from DBS

The protocol developed by Zainabadi *et al.* was used to extract total nucleic acids (DNA and RNA) from the DBS [129]. In short, one entire DBS, which corresponds to 30-50 µL of whole blood, was lysed at 60 °C for 2 h. Nucleic acids were subsequently purified and eluted in 100 µL elution buffer as described elsewhere [130]. The pan-*Plasmodium* spp. 18S ribosomal DNA and RNA molecules were targeted [131] and detected by a highly-sensitive RT-qPCR (herein referred to *Pspp18S* assay) [130]. The Pspp18S assay was analysed qualitatively and samples with Cq values <40 were considered positive. All samples positive for the Pspp18S assay were analysed by species-specific qPCR assays as described previously [132]. Samples positive for P. falciparum were screened for pfhrp2 and/or pfhrp3 deletions using a multiplex qPCR assay [133]. *P. falciparum* parasite density

was determined based on the amplification and detection of the *P. falciparum*-specific single copy gene ribonucleotide reductase R2_e2 [134] by qPCR (*Pfrnr2* assay) [133]. The WHO International Standard for *Plasmodium falciparum* DNA for NAAT-based assays (PfIS) [135] was used to generate a serial dilution in parasite-free whole blood, ranging from 0.01 to 100'000 parasites/µL. Thirty µL of each parasite density was put on a DBS, dried and analysed by the *Pfrnr2* assay. The resulting standard curve, including the slope and y-axis intercept, was used to quantify the parasite densities in the clinical samples. In case the Pfrnr2 assay was negative while the more sensitive Pspp18S assay was positive a parasite density of 1.0 (the analytical limit of detection of the pfrnr2 assay) was assigned to the sample. All qPCR and RT-qPCR assays were run on a Bio-Rad CFX96 Real-Time PCR System (Bio-Rad Laboratories, California, USA). Samples were analyzed in duplicate with positive (PfNF54 DNA) and non-template controls (molecular biology grade H_2O) added to each run.

4.2.3. PeakPCR-Malaria rapid NAAT

The experiments on the peakPCR platform were done with *Plasmodium* spp. cartridges supplied by Diaxxo AG (Zurich, Switzerland). The 20 well cartridges contain all reagents necessary for running a RT-qPCR in preloaded and in lyophilized form. The same oligonucleotide sequences for amplification and detection of *Plasmodium* spp. parasites as for the Pspp18S assay were used. Rapid extraction was performed on DBS punches with 3mm diameter. The DBS punch was submerged in 100 µL of a 5% Chelex (Bio-Rad, California, USA) solution and heated to 95°C for 3 min. The supernatant of the resulting solution was directly used for peakPCR. Briefly, 4µL of eluate per sample were loaded in duplicates onto the 20-well cartridge, covered with paraffin oil (Sigma-Aldrich, St. Louis, USA) and cycled for a duration of 25 minutes (for 45 cycles) in the peakPCR device. Each run contained one well with a positive and one well with a negative control. The cycling parameters for the peakPCR were as follows: reverse transcription of 5 min at 50°C, initial polymerase activation for 1min at 92°C and then 45 cycles of 2 seconds at 92°C and 15 seconds at 55 °C. Raw data was analysed by peakPCR software 2.0 and Cq values were

automatically assigned to the samples. Specimens with amplification and Cq < 40 in 2/2 of replicates were considered positive.

4.3. Results

4.3.1. Parasitological and clinical characteristics of study population

DBS of a total of 47 children were selected for the clinical evaluation of the peakPCR malaria rapid NAAT. The parasitological and clinical characteristics of these children are shown in Table 1. In summary, 31 children were positive for *P. falciparum* and 16 negative for all *Plasmodium* spp. as analysed by the various standard RT-qPCR assays deployed in this diagnostic test evaluation study. Only samples with *P. falciparum* strains without *pfhrp2* and/or *pfhrp3* gene deletions were included since PfHRP2-based RDTs were used for comparison to evaluate the performance of the peakPCR-Malaria rapid NAAT. The *P. falciparum* positive children were stratified according to their parasite density into low (<5000 parasites/µL) and high (≥5000 parasites/µL) infection intensity groups. The children assigned to the high infection intensity group were younger (median age of 13 months), had lower haemoglobin levels and lower red blood cell counts.

Table 6. Characteristics of study population.

Stratification based on parasite density	Parasite density by qPCR (parasites/µL) Median/IQR*	Number of children per group	Age median (range)	Sex (% female)	Haemoglobin median (range) (g/dL)	Red blood cells median (range) (10^6/mm^3)
negative	0	16	5.5 years (6 month – 15 yrs)	50.0%	11.3 (3.6-13.9)	4.1 (0.8-4.9)
Low <5000 per µL	586 (21-2485)	16	3 years (10 month – 14 yrs)	50.0%	7.7 (2.8-12.8)	3.8 (1.0-5.0)
High >5000 per µL	25’800 (11’592-48’371)	15	13 months (2 month - 8 yrs)	53.3%	7.3 (3.9-11.1)	2.9 (1.8-4.6)

*IQR = Interquartile range

4.3.2. Clinical performance of RDT, TBS microscopy and peakPCR-Malaria rapid NAAT

Using, children allocated to the negative (n=16), low intensity (n=16) and high intensity (n=15) infection groups, the clinical performance of the novel peakPCR-Malaria rapid NAAT in comparison to PfHRP2-, panLDH-RDTs as well as TBS microscopy was assessed. The highly sensitive 18S ribosomal rDNA/rRNA RT-qPCR was used the gold standard. The sensitivities/positive percentage agreement (PPA) and the specificity/negative percentage agreement (NPA) are summarized in Table 2. The peakPCR-Malaria rapid NAAT detected all 15 children of the high intensity infection group and 14/16 from the low intensity infection group, resulting in sensitivities of 100% and 87.5%, respectively. The two false-negative children, had parasite densities of 2 and <1 parasites per µL blood, respectively. No false-positive result was recorded for the peakPCR-Malaria rapid NAAT. With 93.3% the PfHRP2-based RDT achieved similar sensitivities for the high intensity infection group. In the low intensity infection group the two peakPCR-Malaria rapid NAAT false-negative children and two additional children were missed by the PfHRP2-based RDT resulting in a sensitivity of 75.0%. Noteworthy, the PfHRP2-RDT showed a reduced specificity with 87.5%. TBS microscopy and the panLDH-RDT showed moderate to high sensitivity among children with high intensity infections and low (TBS microscopy) or moderate (panLDH-RDT) sensitivity in children with low intensity infections.

Table 7. Clinical performance of peakPCR-Malaria rapid NAAT.

	Sensitivity / PPA (95% CI)		**Specificity / NPA (95% CI)**
	Low intensity infection (<5000 parasites/µL) n=16	High intensity infection (>5000 parasites/µL) n=15	- - n=16
TBS microscopy	46.67% (21.27% - 73.41%)	86.67% (59.54% - 98.34%)	100.00% (79.41% - 100.00%)
RDT-PfHRP2	75.00% (47.62% - 92.73%)	93.33% (68.05% - 99.83%)	87.50% (61.65% - 98.45%)
RDT-panLDH	60.00% (32.29% - 83.66%)	80.00% (51.91% - 95.67)	93.75% (69.77% - 99.84%)
peakPCR-Malaria NAAT	87.50% (61.65% - 98.45%)	100.00% (78.20% - 100.00%)	100.00% (79.41% - 100.00%)

4.3.3. Impact of parasite density on sensitivity of diagnostic test performed

When looking at the samples deemed positive by the reference qPCR assay, **Error! Reference source not found.**8 shows that the performance of the different diagnostic tests depends on the parasite density. Although the peakPCR-Malaria rapid NAAT missed the two samples with the lowest parasite densities, the median parasite density was lower than for the PfHRP2-RDT (6826 vs. 8278 parasites/µL), indicating a higher sensitivity. The RDT-panLDH and the TBS microscopy missed samples with parasite densities below 155.7 and 51.5, respectively. A high correlation of Cq values between the peakPCR-Malaria rapid NAAT and the standard Pspp18S RT-qPCR assay was observed (Figure 19).

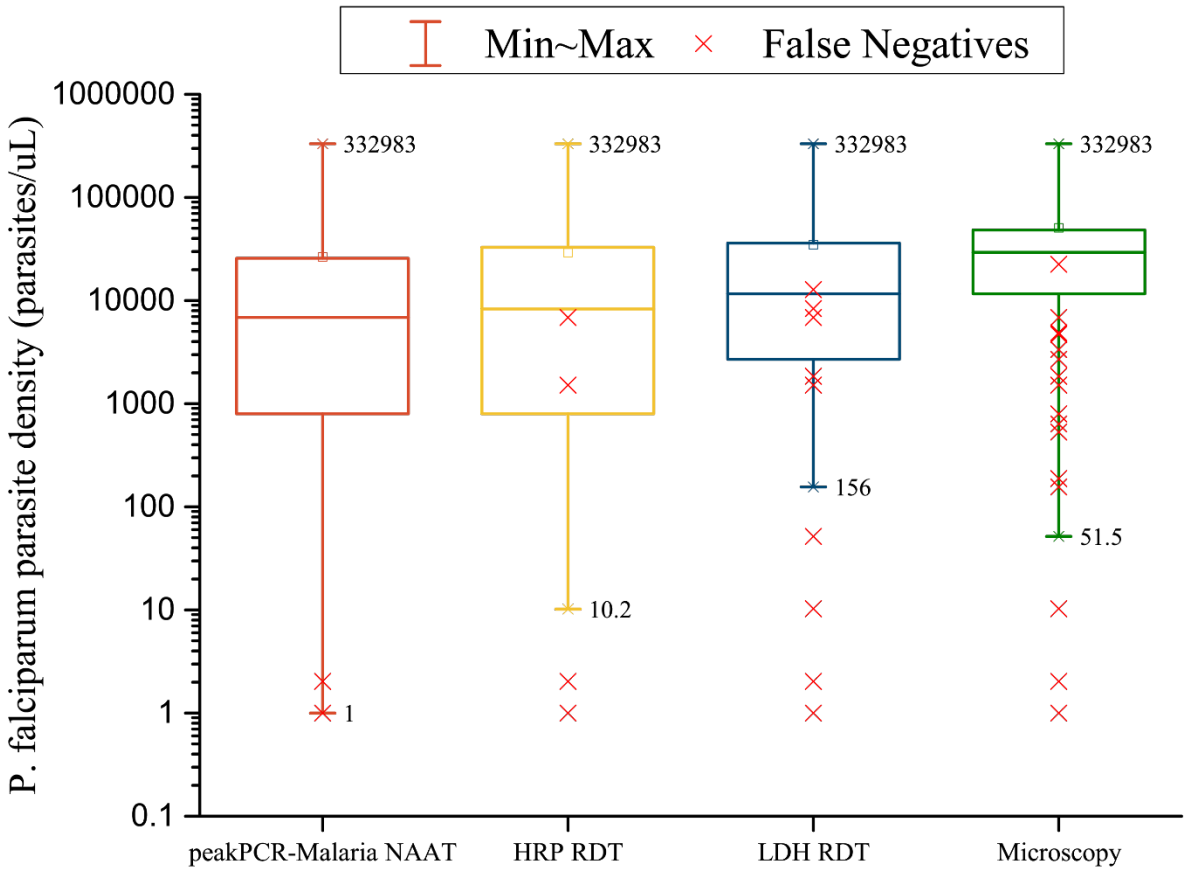

Figure 18. Performance of the different diagnostic tests compared to the parasite densities. Although all methods detected some samples with very low parasite load, the distribution of the boxplot shows where the assays perform reliably.

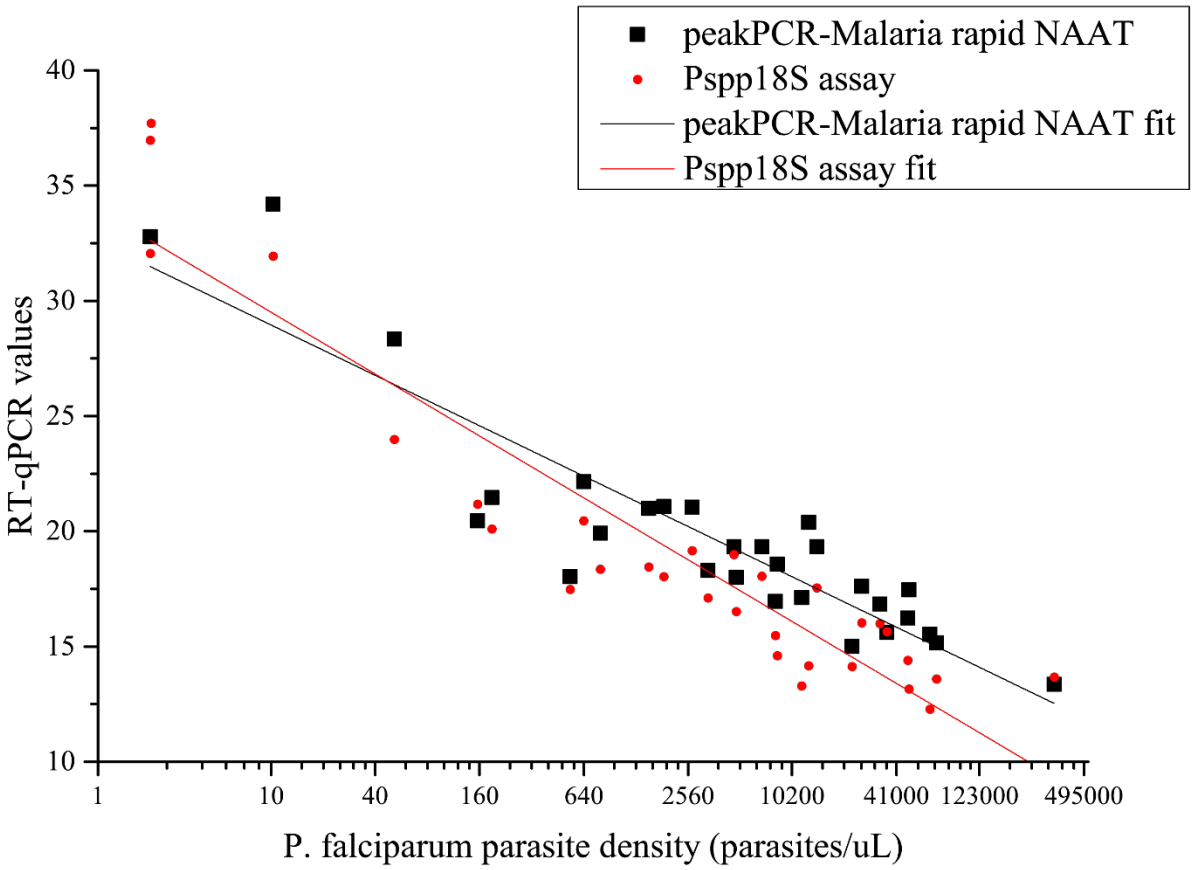

Figure 19. Cq values of peakPCR and the 18S assay on the Bio-Rad CFX96 as a function of the linearized parasite load. Both regressions have slopes of about 1, indicating a PCR efficiency close to 100% for both reactions.

4.4. Discussion

Sensitive and reliable diagnostic tests are the fundamental backbone of healthcare systems. Yet, 47% of the global population has little to no access to diagnostics [136]. We designed and evaluated a novel, rapid NAAT-based diagnostic test for malaria using the low-cost [85] peakPCR platform. Starting from DBS, in less than 30 minutes a diagnostic test for malaria can be conducted with an analytical performance similar to highly-sensitive laboratory-based RT-qPCR assays. The peakPCR-Malaria rapid NAAT is based on cartridges which require little hands-on time as they are preloaded with all RT-qPCR reagents and is therefore well-suited for resource limited settings. The clinical evaluation study we performed revealed that the diagnostic performance of the TBS microscopy and the PfHRP2/panLDH-RDTs is insufficient in terms of sensitivity. Among the 15

symptomatic children, with high infection densities above 5'000 parasites/µL, two were missed by TBS microscopy and one by PfHRP2/panLDH-RDT. The child missed by the PfHRP2/panLDH-RDT cannot be explained by an infection with *P. falciparum* strain carrying *pfhrp2* and/or *pfhrp3* deletions. In addition to lack of sensitivity, also the specificity was reduced. Two out of 16 *Plasmodium* spp. negative children were positive for PfHRP2. False-positive RDTs are common in endemic regions and are likely caused by persisting PfHRP2 antigen circulation post anti-malarial treatment [137], [138]. TBS microscopy missed more than half of the children with low intensity infection (<5000 parasites/µL), while the peakPCR-Malaria rapid NAAT and PfHRP2-RDT showed sensitivities of 87.5% and 75.0%, respectively. The close analysis of the peakPCR-Malaria rapid NAAT shows that the performance is indeed very similar to the state-of-the-art device with the pan-*Plasmodium* 18S rDNA/rRNA RT-qPCR assay. Both assays show a strong correlation between the parasite count and the obtained Cq values. Both linear regression curves coincide closely, indicating that there is no significant inhibition in the rapid extraction procedure. The fact that two samples with low parasite densities were not detected by the peakPCR-Malaria rapid NAAT can be explained by the fact that for the Pspp18 assay an entire DBS with an diameter of approximately 1 cm was used as input for the DNA/RNA extraction, while for the rapid extraction procedure based on Chelex only a single punch with a diameter of 3 mm was used.

4.5. Conclusion

In conclusion, we have established a 30-minute sample-to-result RT-qPCR procedure that delivers results with similar diagnostic performance as state-of-the-art RT-qPCR assays. Until now, molecular diagnostics were only available in centralized laboratories and inaccessible at peripheral health facilities where they were needed most. We are confident that the peakPCR-Malaria rapid

NAAT can bridge this gap and bring highly sensitive malaria testing to the Point-of-Care at peripheral healthcare posts where it's needed most.

5. Conclusion and Outlook

This work presents the potential applications of our *peakPCR* device. In **Chapters 2, 3** and **4**, different uses of the device in different applications are explored and described. The final goal being the accessibility of PCR to a wider audience. Either as a self-testing method, to replace the even more specialized sequencing or to target a disease that causes hundreds of thousands of deaths yearly in developing countries, we are convinced PCR should be for everyone.

The study to use *peakPCR* as a self-testing tool was a great accelerator for the development of the technology because of the extensive feedback recieved from the participants. The first conclusion I was able to come to was that the extraction procedure was still too slow and contained too many steps. An indication that the extraction procedure was indeed complex was that the increase of the success rate of the extraction was strongly dependent on the participants' previous laboratory experience. A second adaptation, based on feedback, that was made during the study was the improvements of the instructions. The final PCR procedure itself had a high success rate of 92%, which shows that minor improvements in the sample loading procedure, deemed the most complicated step, can lead to ultimate success in this approach. In the future, rigorous work needs to be performed either to automatize the sample preparation process, together with the loading, or to reduce the number of processing steps. PCR self-testing will probably not be feasible in the near future, also due to regulatory hurdles, however we have shown that laypeople can potentially learn the use of our device. That could open the door to an intermediate level of healthcare being carried out by doctors, nurses or other people with a basic medical education. Although this may not be the ultimate vision of home-based testing, it would already be a great improvement in the accessibility of rapid PCR testing in settings where the central microbiology laboratories cannot deliver results in the necessary time.

The Sars-Cov-2 variants-of-concern test was the first time a complete external validation was conducted on the device and its consumables. The adaptation of an assay to *peakPCR* that had been developed for a traditional PCR device was easily done within a few days, showing the robustness and versatility of the platform. Not only was the performance of the preloaded cartridges similar to the reference device, but the reaction speed was 50% faster without any optimization of the assay in that regard. The developed assay was able to detect very low amounts of viral load (<10 copies per µL) and was able to detect point mutations reliably, thanks to the LNA modified primers and probes. The fact that PCR can so reliably discern between the smallest mutations opens many doors

for the detection of antibiotic resistances or rare genotypes. Namely that our technology provides much more rapid answers while maintaining the same quality of results as a state-of-the-art PCR device, especially on a wide range of different PCR assays is a key indicator of the powerfulness of the system.

A close collaboration with the Swiss Tropical and Public Health Institute has led to developing an assay for tropical fever diseases, which are still widely under- or misdiagnosed. The currently available tools are insufficient in terms of sensitivity to detect all cases of malaria reliably as I show in **Chapter 3**. The solution I present is a crude extraction without any complicated tools or procedures which is coupled to our fast PCR system. The performance is still significantly better than rapid diagnostic tests and can detect cases of clinical malaria reliably. This study was the first time we applied a rapid extraction procedure from blood which on the one side shows a certain resilience of the developed chemistry to inhibitors and on the other side allows us to test for a wider range of targets like hepatitis or HIV in the future. The fact that the peakPCR system is designed in a lean way without moving parts and is available at relatively low cost predestines it for applications in low- and middle income countries where tropical diseases and especially malaria are widely spread. The thorough analysis we have performed on the blood-based test opens the door for a tropical fever assay testing for malaria, dengue and typhoid fever simultaneously. This work will be tackled together with the Swiss Tropical and Public Health Institute.

In conclusion, I have demonstrated the successful use of the PCR part of peakPCR by laypeople, the rapid and successful development and adaptation of novel assays to the platform and a state-of-the-art performance of the device with its cartridge when using pure DNA/RNA as a starting material. Furthermore, I was able to show that at the cost of a small amount of sensitivity, a very swift and simple protocol to extract DNA/RNA from blood is possible to perform clinically relevant diagnostics that are superior to current rapid test procedures.

6. Appendix

6.1. Appendix Chapter 2

Table S1: Classification of laboratory skills

Participants were divided into 3 cohorts. The classification was carried out based on the total laboratory experience, prior pipetting experience and the time since the last laboratory experience. The table illustrates the constraints for each of the cohorts.

Skill	How long since last time in lab	Total experience
Expert	Less than 2 months	Either daily work or multiple lab courses
Intermediate	Several years	Either daily work or multiple lab courses
Intermediate	Less than 2 months	Only 1 basic lab course (can be chemical)
Novice	Never been in the lab	
Novice	Several years	Only 1 basic lab course (can be chemical)

Figure S1: Example of working space

An example desk where the participants performed the self-test. The desk requires a laptop (1) to view the slideshow of instructions (see Supplemental), a pyramidal peakPCR qPCR device (2) as well as the disposables (3). All liquids were prefilled into labeled tubes in order to reduce the risk of contamination errors (4). Additionally, a camera is placed to record the proceedings of each participant (5).

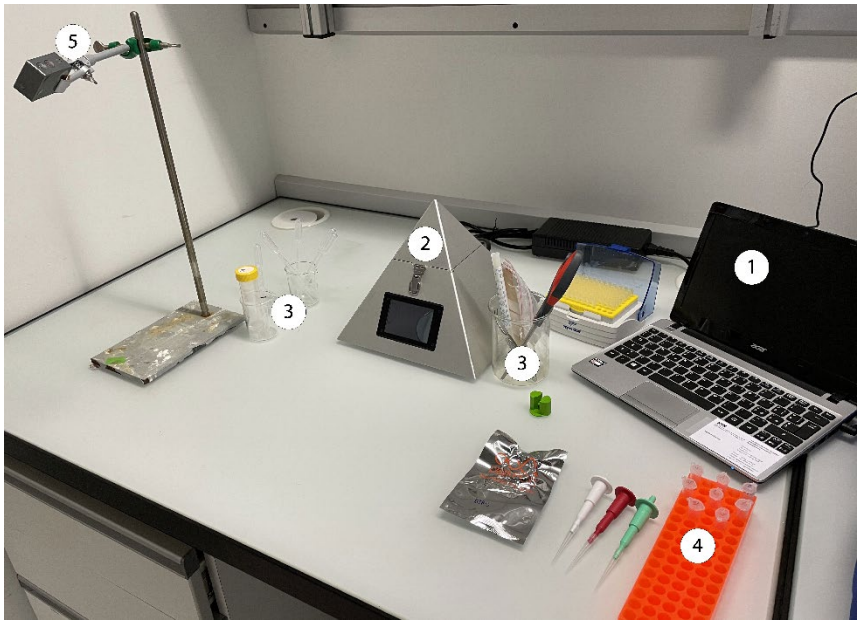

Table S2: peakPCR chip filling layout for Sars-CoV-2

Exact listing of the pre-loading of each position and liquid filling as well as the intended use.

ID	Well position (from top left)	Content	Pre-loaded with	To be filled with	Intended use
S_N1	Row 1, Column 1	SAMPLE	Primers and Probes for N1	Patient's DNA	Test gene N1
S_N2	Row 1, Column 2	SAMPLE	Primers and Probes for N2	Patient's DNA	Test gene N2
S_RP	Row 1, Column 3	SAMPLE	Primers and Probes for RP	Patient's DNA	Test gene RP
P_N1	Row 2, Column 1	NEGATIVE CONTROL	Primers and Probes for N1	Water	Negative control N1
P_N2	Row 2, Column 2	NEGATIVE CONTROL	Primers and Probes for N2	Water	Negative control N2
P_RP	Row 2, Column 3	NEGATIVE CONTROL	Primers and Probes for RP	Water	Negative control RP
N_N1	Row 3, Column 1	POSITIVE CONTROL	Primers and Probes for N1 N1 positive control sequence	Water	Positive control N1
N_N2	Row 3, Column 2	POSITIVE CONTROL	Primers and Probes for N2 N2 positive control sequence	Water	Positive control N2
N_RP	Row 3, Column 3	POSITIVE CONTROL	Primers and Probes for RP RP positive control sequence	Water	Positive control RP

Table S3: peakPCR temperature cycling program

The following temperature program was run in the peakPCR device. Total runtime of a peakPCR experiment was 37 minutes.

reverse transcription	50°C	10min	1x
initial denaturation	95°C	3 min	1x
denaturation	95°C	2 sec	45 x
annealing and elongation	55°C	25 sec	45 x

Table S4: Roche Lightcycler 96 temperature cycling program

The following temperature program was run in the peakPCR device. Total runtime of a Roche Lightcycler 96 experiment was 102 minutes.

reverse transcription	50°C	10min	1x
initial denaturation	95°C	5 min	1x
denaturation	95°C	15 sec	45 x
annealing and elongation	55°C	60 sec	45 x

Table S5: Age, Gender, Educational Background and Skill Classification of all Participants

The participants filled out a questionnaire before being invited and this table shows the distribution of age, gender, educational background and skill classification of all participants. The gender distribution was about 50/50, while most of the participants were younger than 26 years. Almost all participants had at least a finished high-school degree. The cohorts were almost exactly populated into thirds.

Characteristic	n(%)
Age (years)	
18-21	114 (43.3)
22-25	81 (30.8)
26-29	44 (16.7)
30-34	10 (3.8)
35-39	6 (2.3)
>40	8 (3)
Current gender	
Male	142 (54)
Female	120 (45.6)
Other	1 (0.4)
Education	
PhD	7 (2.7)
Master degree	51 (19.4)
Bachelor degree	55 (20.9)
High school degree	139 (52.9)
College degree	3 (1.1)
Apprenticeship	8 (3)
None	0 (0)
Laboratory skills	
Expert	93 (35.4)
Intermediate	91 (34.6)
Novice	79 (30)

Figure S2: Magnetic holder for the beads separation

Image of the magnetic holder for the beads separation. The 3D printed adapter holds a tube and the magnet is placed so that the beads are positioned on the sidewall and thus easily separated from the supernatant.

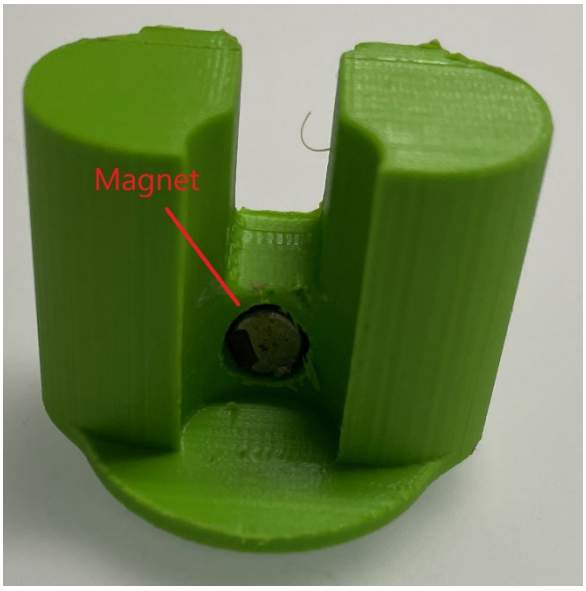

Figure S3: Distribution of participants preferring to do the test themselves compared to the success rate of extraction

The success rate of the extraction increases with prior laboratory experience. However, the participants with intermediate experience are the most confident in the test they performed and would prefer to do it themselves.

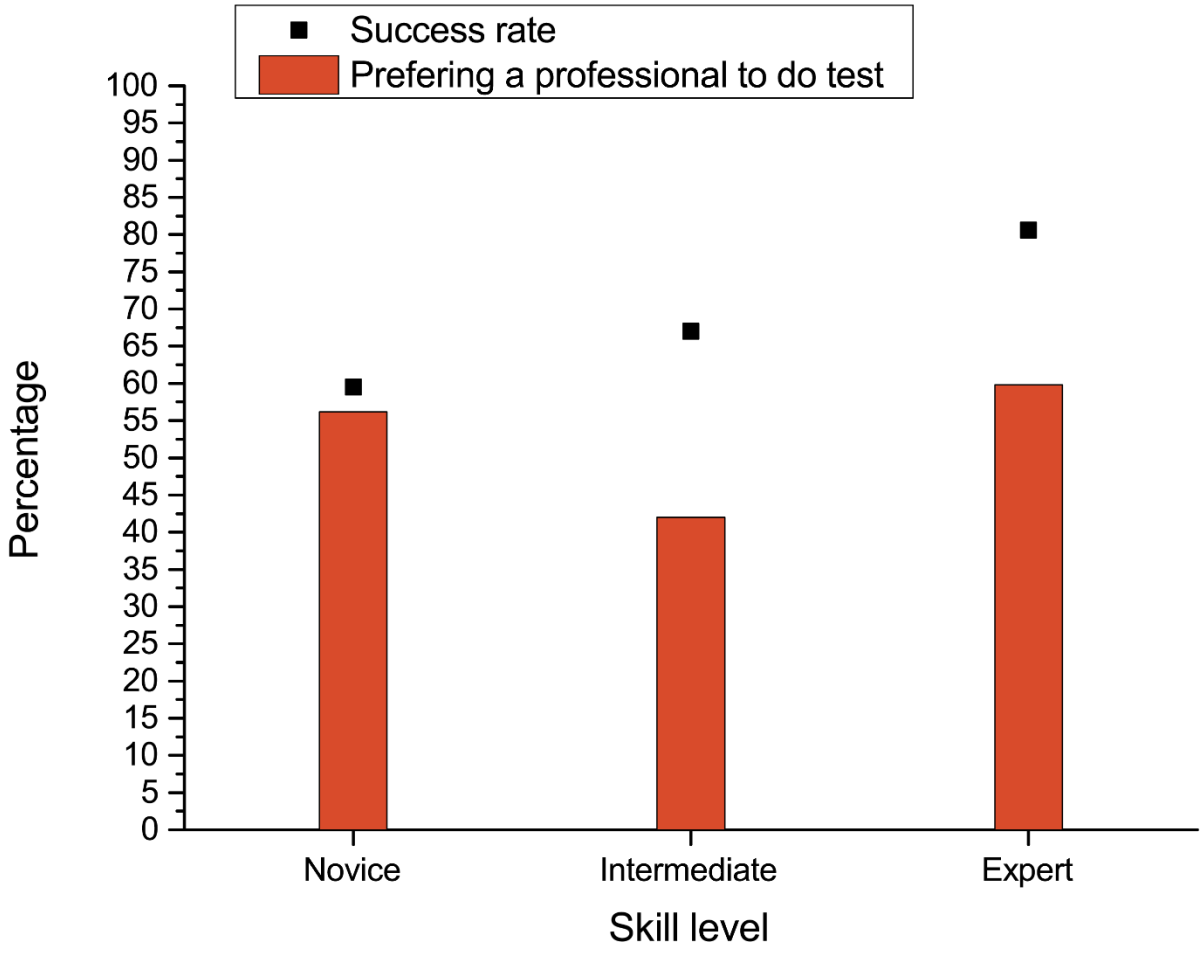

6.2. Appendix Chapter 3

Figure S4: Sequence of synthetic spike gene fragment A 1869 bp long synthetic Sars-CoV-2 spike gene fragment (genome position 21,557-23,434 bp), based on the sequence of B.1.1.7 was synthesized by Eurofins Genomics, Konstanz, Germany.

```
   1 gaacaatgtt tgtttttctt gttttattgc cactagtctc tagtcagtgt gttaatctta
  61 caaccagaac tcaattaccc cctgcataca ctaattcttt cacacgtggt gtttattacc
 121 ctgacaaagt tttcagatcc tcagttttac attcaactca ggacttgttc ttacctttct
 181 tttccaatgt tacttggttc catgctatct ctgggaccaa tggtactaag aggtttgata
 241 accctgtcct accatttaat gatggtgttt attttgcttc actgagaag tctaacataa
 301 taagaggctg gatttttggt actactttag attcgaagac ccagtcccta cttattgtta
 361 ataacgctac taatgttgtt attaaagtct gtgaatttca attttgtaat gatccatttt
 421 tgggtgttta ccacaaaaac aacaaaagtt ggatggaaag tgagttcaga gtttattcta
 481 gtgcgaataa ttgcactttt gaatatgtct ctcagccttt tcttatggac cttgaaggaa
 541 aacagggtaa tttcaaaaat cttagggaat ttgtgtttaa gaatattgat ggttatttta
 601 aaatatattc taagcacacg cctattaatt tagtgcgtga tctccctcag ggtttttcgg
 661 ctttagaacc attggtagat ttgccaatag gtattaacat cactaggttt caaactttac
 721 ttgctttaca tagaagttat ttgactcctg gtgattcttc ttcaggttgg acagctggtg
 781 ctgcagctta ttatgtgggt tatcttcaac ctaggacttt tctattaaaa tataatgaaa
 841 atggaaccat tacagatgct gtagactgtg cacttgaccc tctctcagaa acaaagtgta
 901 cgttgaaatc cttcactgta gaaaaaggaa tctatcaaac ttctaacttt agagtccaac
 961 caacagaatc tattgttaga tttcctaata ttacaaactt gtgccctttt ggtgaagttt
1021 ttaacgccac cagatttgca tctgtttatg cttggaacag gaagagaatc agcaactgtg
1081 ttgctgatta ttctgtccta tataattccg catcattttc acttttaag tgttatggag
1141 tgtctcctac taaattaaat gatctctgct ttactaatgt ctatgcagat tcatttgtaa
1201 ttagaggtga tgaagtcaga caaatcgctc cagggcaaac tggaaagatt gctgattata
1261 attataaatt accagatgat tttacaggct gcgttatagc ttggaattct aacaatcttg
1321 attctaaggt tggtggtaat tataattacc tgtatagatt gtttaggaag tctaatctca
1381 aacctttga gagagatatt tcaactgaaa tctatcaggc cggtagcaca ccttgtaatg
1441 gtgttgaagg ttttaattgt tactttcctt tacaatcata tggtttccaa cccacttatg
1501 gtgttggtta ccaaccatac agagtagtag tactttcttt tgaacttcta catgcaccag
1561 caactgtttg tggacctaaa aagtctacta atttggttaa aaacaaatgt gtcaatttca
1621 acttcaatgg tttaacaggc acaggtgttc ttactgagtc taacaaaaag tttctgcctt
1681 tccaacaatt tggcagagac attgatgaca ctactgatgc tgtccgtgat ccacagacac
1741 ttgagattct tgacattaca ccatgttctt ttggtggtgt cagtgttata acaccaggaa
1801 caaatacttc taaccaggtt gctgttcttt atcagggtgt taactgcaca gaagtccctg
1861 ttgctattc
```

Figure S5: Synthetic spike gene serial dilution experiments for HV69/70 and N501Y assays.

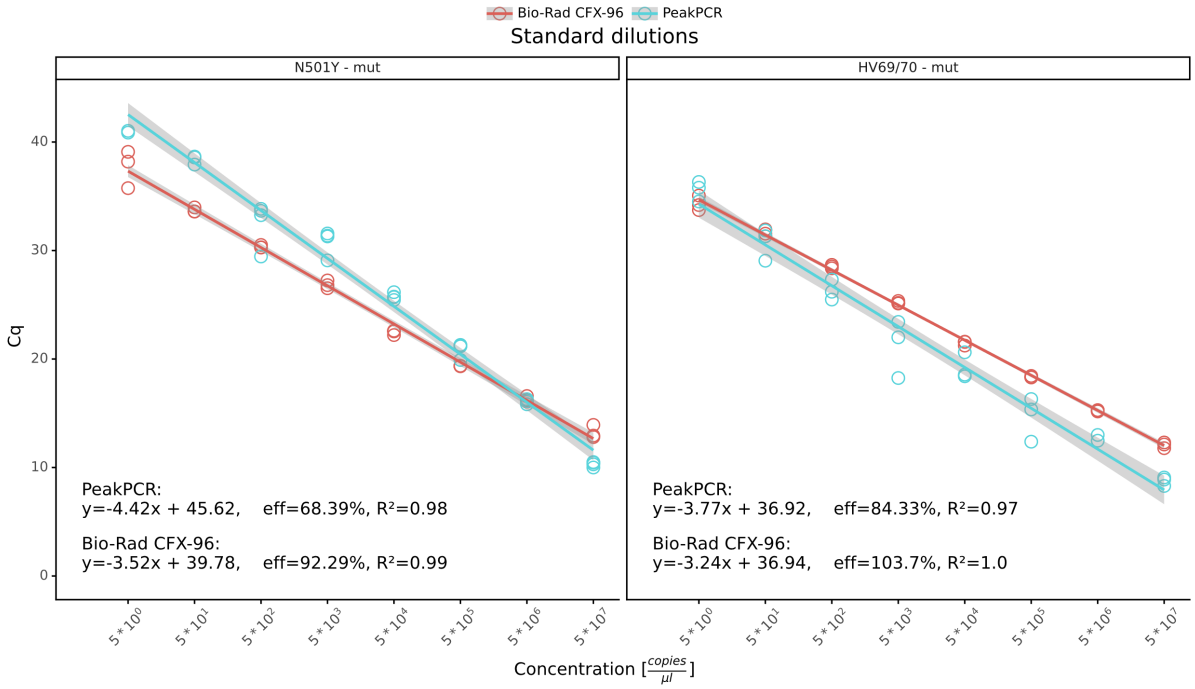

Figure S6: Comparison of lyophilized reagents with non-lyophilized standard RT-qPCR reagents on the *peak*PCR device

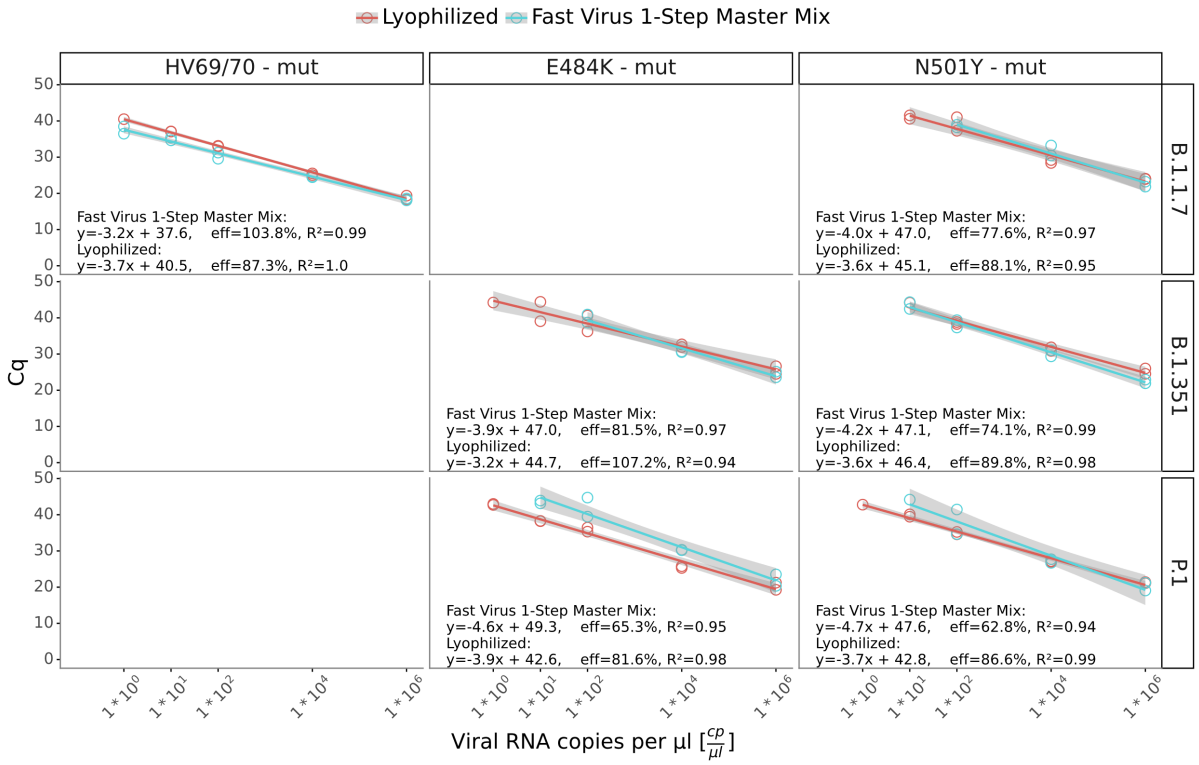

References

[1] J. D. WATSON and F. H. C. CRICK, “Molecular Structure of Nucleic Acids: A Structure for Deoxyribose Nucleic Acid,” *Nature*, vol. 171, no. 4356, pp. 737–738, Apr. 1953, doi: 10.1038/171737a0.

[2] I. R. Lehman, M. J. Bessman, E. S. Simms, and A. Kornberg, “Enzymatic Synthesis of Deoxyribonucleic Acid,” *J. Biol. Chem.*, vol. 233, no. 1, pp. 163–170, Jul. 1958, doi: 10.1016/S0021-9258(19)68048-8.

[3] A. Chien, D. B. Edgar, and J. M. Trela, “Deoxyribonucleic acid polymerase from the extreme thermophile Thermus aquaticus,” *J. Bacteriol.*, vol. 127, no. 3, pp. 1550–1557, Sep. 1976, doi: 10.1128/jb.127.3.1550-1557.1976.

[4] Invitrogen, “SuperScript® One-Step RT-PCR System with Platinum® Taq DNA Polymerase,” no. 12574, pp. 1–4, 2001, [Online]. Available: https://www.thermofisher.com/order/catalog/product/12574018#/12574018.

[5] K. B. Mullis, “The unusual origin of the polymerase chain reaction,” *Sci. Am.*, vol. 262, no. 4, pp. 56–65, 1990, doi: 10.1038/scientificamerican0490-56.

[6] C. W. Tang, Yi-Wei Stratton, *Advanced Techniques in Diagnostic Microbiology*. Springer, 2006.

[7] Y.-W. Tang, G. W. Procop, and D. H. Persing, “Molecular diagnostics of infectious diseases,” *Clin. Chem.*, vol. 43, no. 11, pp. 2021–2038, Nov. 1997, doi: 10.1093/clinchem/43.11.2021.

[8] M. Johnson, “Pandemic Pushes Handheld qPCR Devices Closer to Commercialization,” 2021. https://www.360dx.com/pcr/pandemic-pushes-handheld-qpcr-devices-closer-commercialization.

[9] J. Watson, “Double Helix.” Orion Publishing Co., 2010, [Online]. Available: https://biologydictionary.net/wp-content/uploads/2020/05/DNA_double_helix_structure_.jpg.

[10] A. Ahmad and J. Ghasemi, “New buffers to improve the quantitative real-time polymerase chain reaction,” *Biosci. Biotechnol. Biochem.*, vol. 71, no. 8, pp. 1970–1978, 2007, doi: 10.1271/bbb.70164.

[11] Enzyklop, “CC BY-SA 3.0.” Wikimedia Commons, 2014.

[12] N. Paul, J. Shum, and T. Le, “Hot Start PCR,” 2010, pp. 301–318.

[13] M. McPherson and S. Møller, *PCR*. Taylor & Francis, 2006.

[14] A. Tiselius, “A new apparatus for electrophoretic analysis of colloidal mixtures,” *Trans. Faraday Soc.*, vol. 33, p. 524, 1937, doi: 10.1039/tf9373300524.

[15] J. Sambrook and W. Russel, D, “Molecular Cloning, 3-Volume Set : A Laboratory Manual,” *Cold Spring Harboc Laboratory Press*, vol. 3. p. 999, 2000, [Online]. Available: http://www.ncbi.nlm.nih.gov/pubmed/24532655.

[16] W. A. Franklin and J. D. Locker, “Ethidium bromide: a nucleic acid stain for tissue section.,” *J. Histochem. Cytochem.*, vol. 29, no. 4, pp. 572–576, Apr. 1981, doi: 10.1177/29.4.6166660.

[17] H. Zipper, “Investigations on DNA intercalation and surface binding by SYBR Green I, its structure determination and methodological implications,” *Nucleic Acids Res.*, vol. 32, no. 12, pp. e103–e103, Jul. 2004, doi: 10.1093/nar/gnh101.

[18] Roche, “KAPA SYBR FAST qPCR Kits,” 2021. https://sequencing.roche.com/en/products-solutions/products/qpcr/kapa-sybr-fast/ordering.html.

[19] K. McCaustland, “Real-Time PCR: An Essential Guide,” *Emerg. Infect. Dis.*, vol. 11, no. 1, pp. 185–186, Jan. 2005, doi: 10.3201/eid1101.040896.

[20] B. Juskowiak, “Nucleic acid-based fluorescent probes and their analytical potential,” *Anal. Bioanal. Chem.*, vol. 399, no. 9, pp. 3157–3176, Mar. 2011, doi: 10.1007/s00216-010-4304-5.

[21] E. Navarro, G. Serrano-Heras, M. J. Castaño, and J. Solera, “Real-time PCR detection chemistry,” *Clin. Chim. Acta*, vol. 439, pp. 231–250, 2015, doi: 10.1016/j.cca.2014.10.017.

[22] P. M. Holland, R. D. Abramson, R. Watson, and D. H. Gelfand, “Detection of specific polymerase chain reaction product by utilizing the 5’----3’ exonuclease activity of Thermus aquaticus DNA polymerase.,” *Proc. Natl. Acad. Sci.*, vol. 88, no. 16, pp. 7276–7280, Aug. 1991, doi: 10.1073/pnas.88.16.7276.

[23] O. Henegariu, S. R. Dlouhy, G. H. Vance, and P. H. Vogt, “Multiplex PCR : Critical Parameters and,” *Biotechniques*, vol. 511, no. September, pp. 504–511, 1997.

[24] U. E. Gibson, C. A. Heid, and P. M. Williams, “A novel method for real time quantitative RT-PCR.,” *Genome Res.*, vol. 6, no. 10, pp. 995–1001, Oct. 1996, doi: 10.1101/gr.6.10.995.

[25] L. Jansson and J. Hedman, “Challenging the proposed causes of the PCR plateau phase,” *Biomol. Detect. Quantif.*, vol. 17, p. 100082, Mar. 2019, doi: 10.1016/j.bdq.2019.100082.

[26] A. N. Spiess, C. Feig, and C. Ritz, “Highly accurate sigmoidal fitting of real-time PCR data by introducing a parameter for asymmetry,” *BMC Bioinformatics*, vol. 9, pp. 1–12, 2008, doi: 10.1186/1471-2105-9-221.

[27] D. C. Rio, “Reverse Transcription–Polymerase Chain Reaction,” *Cold Spring Harb. Protoc.*, vol. 2014, no. 11, p. pdb.prot080887, Nov. 2014, doi: 10.1101/pdb.prot080887.

[28] J. W. Larrick, “Message amplification phenotyping (MAPPing) — principles, practice and potential,” *Trends Biotechnol.*, vol. 10, pp. 146–152, 1992, doi: 10.1016/0167-7799(92)90202-7.

[29] C. Haddar, P. O. Verhoeven, T. Bourlet, B. Pozzetto, and S. Pillet, “Brief comparative evaluation of six open one-step RT-qPCR mastermixes for the detection of SARS-CoV-2 RNA using a Taqman probe,” *J. Clin. Virol.*, vol. 132, p. 104636, Nov. 2020, doi: 10.1016/j.jcv.2020.104636.

[30] T. Remans, K. Smeets, K. Opdenakker, D. Mathijsen, J. Vangronsveld, and A. Cuypers, “Normalisation of real-time RT-PCR gene expression measurements in Arabidopsis thaliana exposed to increased metal concentrations,” *Planta*, vol. 227, no. 6, pp. 1343–1349, May 2008, doi: 10.1007/s00425-008-0706-4.

[31] B. Alberts *et al.*, *Molecular Biology of the Cell*, 6th ed. W. W. Norton & Co., 2020.

[32] E. M. Wagner, “Monitoring Gene Expression: Quantitative Real-Time RT-PCR,” 2013, pp. 19–45.

[33] T. D. Schmittgen and B. A. Zakrajsek, “Effect of experimental treatment on housekeeping gene expression: validation by real-time, quantitative RT-PCR,” *J. Biochem. Biophys. Methods*, vol. 46, no. 1–2, pp. 69–81, Nov. 2000, doi: 10.1016/S0165-022X(00)00129-9.

[34] R. E. Levin, “The Application of Real-Time PCR to Food and Agricultural Systems. A Review,” *Food Biotechnol.*, vol. 18, no. 1, pp. 97–133, Jan. 2004, doi: 10.1081/FBT-120030386.

[35] H. Karch and T. Meyer, “Single primer pair for amplifying segments of distinct Shiga-like-toxin genes by polymerase chain reaction,” *J. Clin. Microbiol.*, vol. 27, no. 12, pp. 2751–2757, Dec. 1989, doi: 10.1128/jcm.27.12.2751-2757.1989.

[36] C.-D. Kaptchouang Tchatchouang *et al.*, “Listeriosis Outbreak in South Africa: A Comparative Analysis with Previously Reported Cases Worldwide,” *Microorganisms*, vol. 8, no. 1, p. 135, Jan. 2020, doi: 10.3390/microorganisms8010135.

[37] FDA, “Salmonella sampling plan,” *FDA*, pp. 184–205, 2015.

[38] N. Martínez, M. C. Martín, A. Herrero, M. Fernández, M. A. Alvarez, and V. Ladero, “qPCR as a powerful tool for microbial food spoilage quantification: Significance for food quality,” *Trends Food Sci. Technol.*, vol. 22, no. 7, pp. 367–376, Jul. 2011, doi: 10.1016/j.tifs.2011.04.004.

[39] B. Röder, K. Frühwirth, C. Vogl, M. Wagner, and P. Rossmanith, “Impact of Long-Term Storage on Stability of Standard DNA for Nucleic Acid-Based Methods,” *J. Clin. Microbiol.*, vol. 48, no. 11, pp. 4260–4262, Nov. 2010, doi: 10.1128/JCM.01230-10.

[40] “Created with BioRender.com.” .

[41] C. James, *Brief 42: Global Status of Commercialized Biotech/GM Crops: 2010*. 2010.

[42] EU, “Regulation (EC) No 1829/2003 of the European Parliament and of the council on genetically modified food and feed,” *Off. J. Eur. Union*, vol. L 268, pp. 1–23, 2003, [Online]. Available: http://eur-lex.europa.eu/legal-content/en/ALL/?uri=CELEX:32003R1829.

[43] EC (European Comission), “Commission implementing regulation (EU) No 503/2013 of 3 April 2013 on applications for authorisation of genetically modified food and feed in accordance with Regulation (EC) No 1829/2003 of the European Parliament and of the Council and amending Commissi,” *Off. J. Eur. Union*, vol. L, pp. 1–157, 2013, [Online]. Available: https://lexparency.org/eu/32013R0503/.

[44] Eu, “GMOMETHODS,” 2021. https://gmo-crl.jrc.ec.europa.eu/gmomethods/.

[45] M. A. Fraiture, P. Herman, I. Taverniers, M. De Loose, D. Deforce, and N. H. Roosens, “Current and New Approaches in GMO Detection: Challenges and Solutions,” *Biomed Res. Int.*, vol. 2015, no. Table 1, 2015, doi: 10.1155/2015/392872.

[46] A. Holst-Jensen *et al.*, “Detecting un-authorized genetically modified organisms (GMOs) and derived materials,” *Biotechnol. Adv.*, vol. 30, no. 6, pp. 1318–1335, Nov. 2012, doi: 10.1016/j.biotechadv.2012.01.024.

[47] K. Rudi, M. Kroken, O. J. Dahlberg, A. Deggerdal, K. S. Jakobsen, and F. Larsen, “Rapid, universal method to isolate PCR-ready DNA using magnetic beads,” *Biotechniques*, vol. 22, no. 3, pp. 506–511, 1997, doi: 10.2144/97223rr01.

[48] A. K. Yetisen, M. S. Akram, and C. R. Lowe, “Paper-based microfluidic point-of-care diagnostic devices,” *Lab Chip*, vol. 13, no. 12, pp. 2210–2251, 2013, doi: 10.1039/c3lc50169h.

[49] C. Sheridan, “Fast, portable tests come online to curb coronavirus pandemic,” *Nat. Biotechnol.*, vol. 38, no. 5, pp. 515–518, May 2020, doi: 10.1038/d41587-020-00010-2.

[50] K. M. Koczula and A. Gallotta, “Lateral flow assays,” *Essays Biochem.*, vol. 60, no. 1, pp. 111–120, Jun. 2016, doi: 10.1042/EBC20150012.

[51] S. Mankarious *et al.*, “The half-lives of IgG subclasses and specific antibodies in patients with primary immunodeficiency who are receiving intravenously administered immunoglobulin.,” *J. Lab. Clin. Med.*, vol. 112, no. 5, pp. 634–640, Nov. 1988.

[52] N. Doria-Rose *et al.*, “Antibody Persistence through 6 Months after the Second Dose of mRNA-1273 Vaccine for Covid-19,” *N. Engl. J. Med.*, vol. 384, no. 23, pp. 2259–2261, Jun. 2021, doi: 10.1056/NEJMc2103916.

[53] A. Anantharajah *et al.*, “How to choose the right real-time RT-PCR primer sets for the SARS-CoV-2 genome detection?,” *J. Virol. Methods*, vol. 295, pp. 1–8, 2021, doi: 10.1016/j.jviromet.2021.114197.

[54] Y. Jung *et al.*, “Comparative Analysis of Primer–Probe Sets for RT-qPCR of COVID-19 Causative Virus (SARS-CoV-2),” *ACS Infect. Dis.*, vol. 6, no. 9, pp. 2513–2523, Sep. 2020, doi: 10.1021/acsinfecdis.0c00464.

[55] H. Jayamohan *et al.*, “SARS-CoV-2 pandemic: a review of molecular diagnostic tools including sample collection and commercial response with associated advantages and limitations,” *Anal. Bioanal. Chem.*, vol. 413, no. 1, pp. 49–71, 2021, doi: 10.1007/s00216-020-02958-1.

[56] R. Wölfel *et al.*, “Virological assessment of hospitalized patients with COVID-2019,” *Nature*, vol. 581, no. 7809, pp. 465–469, May 2020, doi: 10.1038/s41586-020-2196-x.

[57] M. J. Mina, T. E. Peto, M. García-Fiñana, M. G. Semple, and I. E. Buchan, “Clarifying the evidence on SARS-CoV-2 antigen rapid tests in public health responses to COVID-19,” *Lancet*, vol. 397, no. 10283, pp. 1425–1427, Apr. 2021, doi: 10.1016/S0140-6736(21)00425-6.

[58] J. J. Deeks and A. E. Raffle, “Lateral flow tests cannot rule out SARS-CoV-2 infection,” *BMJ*, vol. 371, Dec. 2020, doi: 10.1136/BMJ.M4787.

[59] L. Porte *et al.*, “Evaluation of a novel antigen-based rapid detection test for the diagnosis of SARS-CoV-2 in respiratory samples,” *Int. J. Infect. Dis.*, vol. 99, pp. 328–333, Oct. 2020, doi: 10.1016/J.IJID.2020.05.098.

[60] D. K. Flaherty, “Antibodies,” in *Immunology for Pharmacy*, Elsevier, 2012, pp. 70–78.

[61] L. Gummery, S. Jallow, A. G. Raftery, E. Bennet, J. Rodgers, and D. G. M. Sutton, “Comparison of loop-mediated isothermal amplification (LAMP) and PCR for the diagnosis of infection with Trypanosoma brucei ssp. in equids in The Gambia,” *PLoS One*, vol. 15, no. 8, p. e0237187, Aug. 2020, doi: 10.1371/journal.pone.0237187.

[62] M. Jevšnik, L. Lusa, T. Uršič, U. Glinšek Biškup, and M. Petrovec, “Detection of herpes simplex and varicella-zoster virus from skin lesions: comparison of RT-PCR and

isothermal amplification for rapid identification," *Diagn. Microbiol. Infect. Dis.*, vol. 97, no. 2, p. 115015, Jun. 2020, doi: 10.1016/j.diagmicrobio.2020.115015.

[63] E. T. Beck, W. Paar, L. Fojut, J. Serwe, and R. R. Jahnke, "Comparison of the Quidel Sofia SARS FIA Test to the Hologic Aptima SARS-CoV-2 TMA Test for Diagnosis of COVID-19 in Symptomatic Outpatients," *J. Clin. Microbiol.*, vol. 59, no. 2, Jan. 2021, doi: 10.1128/JCM.02727-20.

[64] Y. Shabi *et al.*, "Comparison of two automated methods for detection and differentiation of herpes simplex virus in clinical specimens," *J. Clin. Virol.*, vol. 117, pp. 85–88, Aug. 2019, doi: 10.1016/j.jcv.2019.04.010.

[65] S. H. Hodgson *et al.*, "Increased sample volume and use of quantitative reverse-transcription PCR can improve prediction of liver-to-blood inoculum size in controlled human malaria infection studies," *Malar. J.*, vol. 14, no. 1, p. 33, Dec. 2015, doi: 10.1186/s12936-015-0541-6.

[66] M. Intelligence, "MOLECULAR DIAGNOSTICS MARKET - GROWTH, TRENDS, COVID-19 IMPACT, AND FORECASTS (2021 - 2026)," 2021. [Online]. Available: https://www.mordorintelligence.com/industry-reports/molecular-diagnostics-market.

[67] WHO, "Molecular diagnostics Integration Global Meeting Report," no. July, p. 20, 2019, [Online]. Available: https://apps.who.int/iris/handle/10665/331708.

[68] "Analysenliste," no. 01.07. Bundesamt für Gesundheit, 2021.

[69] G. J. Kost, "Guidelines for point-of-care testing. Improving patient outcomes.," *Am. J. Clin. Pathol.*, vol. 104, no. 4 Suppl 1, pp. S111-27, Oct. 1995.

[70] V. Gubala, L. F. Harris, A. J. Ricco, M. X. Tan, and D. E. Williams, "Point of Care Diagnostics: Status and Future," *Anal. Chem.*, vol. 84, no. 2, pp. 487–515, Jan. 2012, doi: 10.1021/ac2030199.

[71] S. Vashist, "Point-of-Care Diagnostics: Recent Advances and Trends," *Biosensors*, vol. 7, no. 4, p. 62, Dec. 2017, doi: 10.3390/bios7040062.

[72] M. Gregorini, G. Mikutis, R. N. Grass, and W. J. Stark, "Small-Size Polymerase Chain Reaction Device with Improved Heat Transfer and Combined Feedforward/Feedback

Control Strategy," *Ind. Eng. Chem. Res.*, vol. 58, no. 22, pp. 9665–9674, 2019, doi: 10.1021/acs.iecr.9b01209.

[73] WHO, "Tracking SARS-CoV-2 variants," 2021. https://www.who.int/en/activities/tracking-SARS-CoV-2-variants/.

[74] P. Zhou *et al.*, "A pneumonia outbreak associated with a new coronavirus of probable bat origin," *Nature*, vol. 579, no. 7798, pp. 270–273, 2020, doi: 10.1038/s41586-020-2012-7.

[75] IMF, "A Crisis Like No Other, An Uncertain Recovery," *World Econ. Outlook Updat.*, no. June 2020, pp. 1–20, 2020.

[76] K. M. Gostic, A. C. R. Gomez, R. O. Mummah, A. J. Kucharski, and J. O. Lloyd-Smith, "Estimated effectiveness of symptom and risk screening to prevent the spread of COVID-19," *Elife*, vol. 9, pp. 1–18, 2020, doi: 10.7554/eLife.55570.

[77] D. T. A. Ghebreyesus, "Opening Remarks of the director general of the WHO on March 16," [Online]. Available: https://www.who.int/dg/speeches/detail/who-director-general-s-opening-remarks-at-the-media-briefing-on-covid-19---16-march-2020.

[78] World Health Organisation, "Strategic preparedness and response plan," no. April, p. 18, 2020.

[79] M. Gandhi, D. S. Yokoe, and D. V. Havlir, "Asymptomatic transmission, the achilles' heel of current strategies to control Covid-19," *N. Engl. J. Med.*, vol. 382, no. 22, pp. 2158–2160, 2020, doi: 10.1056/NEJMe2009758.

[80] N. Sethuraman, S. S. Jeremiah, and A. Ryo, "Interpreting Diagnostic Tests for SARS-CoV-2," *JAMA - J. Am. Med. Assoc.*, vol. 323, no. 22, pp. 2249–2251, 2020, doi: 10.1001/jama.2020.8259.

[81] X. Wang *et al.*, "Comparison of nasopharyngeal and oropharyngeal swabs for SARS-CoV-2 detection in 353 patients received tests with both specimens simultaneously," *Int. J. Infect. Dis.*, vol. 94, pp. 107–109, 2020, doi: 10.1016/j.ijid.2020.04.023.

[82] K. Uhteg *et al.*, "Comparing the analytical performance of three SARS-CoV-2 molecular diagnostic assays," *J. Clin. Virol.*, vol. 127, no. April, p. 104384, 2020, doi: 10.1016/j.jcv.2020.104384.

[83] M. Döhla *et al.*, “Rapid point-of-care testing for SARS-CoV-2 in a community screening setting shows low sensitivity,” *Public Health*, vol. 182, pp. 170–172, 2020, doi: 10.1016/j.puhe.2020.04.009.

[84] Bundesamt für Gesundheit Schweiz, “Test results Switzerland Corona.” https://www.bag.admin.ch/dam/bag/de/dokumente/mt/k-und-i/aktuelle-ausbrueche-pandemien/2019-nCoV/covid-19-basisdaten-labortests.xlsx.download.xlsx/Dashboard_3_COVID19_labtests_positivity.xlsx (accessed Jan. 13, 2021).

[85] S. Hosch *et al.*, “Rapid identification of Sars-CoV-2 variants of concern using the portable peakPCR platform,” *medRxiv*, p. 2021.05.21.21256124, Jan. 2021, doi: 10.1101/2021.05.21.21256124.

[86] E. Dong, H. Du, and L. Gardner, “An interactive web-based dashboard to track COVID-19 in real time,” *The Lancet Infectious Diseases*, vol. 20, no. 5. Lancet Publishing Group, pp. 533–534, May 2020, doi: 10.1016/S1473-3099(20)30120-1.

[87] R. P. Walensky, H. T. Walke, and A. S. Fauci, “SARS-CoV-2 Variants of Concern in the United States—Challenges and Opportunities,” *JAMA*, Feb. 2021, doi: 10.1001/jama.2021.2294.

[88] B. B. Oude Munnink *et al.*, “Rapid SARS-CoV-2 whole-genome sequencing and analysis for informed public health decision-making in the Netherlands,” *Nat. Med.*, vol. 26, no. 9, pp. 1405–1410, Sep. 2020, doi: 10.1038/s41591-020-0997-y.

[89] W. H. Organization, *Genomic sequencing of SARS-CoV-2: a guide to implementation for maximum impact on public health, 8 January 2021*. World Health Organization, 2021.

[90] N. Zhu *et al.*, “A Novel Coronavirus from Patients with Pneumonia in China, 2019,” *N. Engl. J. Med.*, vol. 382, no. 8, pp. 727–733, Feb. 2020, doi: 10.1056/nejmoa2001017.

[91] Q. Li *et al.*, “The Impact of Mutations in SARS-CoV-2 Spike on Viral Infectivity and Antigenicity,” *Cell*, vol. 182, no. 5, pp. 1284-1294.e9, Sep. 2020, doi: 10.1016/j.cell.2020.07.012.

[92] B. Korber *et al.*, “Tracking Changes in SARS-CoV-2 Spike: Evidence that D614G

Increases Infectivity of the COVID-19 Virus," *Cell*, vol. 182, no. 4, pp. 812-827.e19, Aug. 2020, doi: 10.1016/j.cell.2020.06.043.

[93] "Updated rapid risk assessment from ECDC on the risk related to the spread of new SARS-CoV-2 variants of concern in the EU/EEA – first update," *Eurosurveillance*, vol. 26, no. 3, p. 2101211, Jan. 2021, doi: 10.2807/1560-7917.ES.2021.26.3.2101211.

[94] C. S. Peter Horby, Catherine Huntley, Nick Davies, John Edmunds, Neil Ferguson, Graham Medley, "SAGE Meeting paper 2021/01/21." .

[95] H. Tegally *et al.*, "Emergence and rapid spread of a new severe acute respiratory syndrome-related coronavirus 2 (SARS-CoV-2) lineage with multiple spike mutations in South Africa," *medRxiv*, vol. 10. medRxiv, p. 2020.12.21.20248640, Dec. 2020, doi: 10.1101/2020.12.21.20248640.

[96] E. C. S. on behalf of C. G. N. Nuno R. Faria, Ingra Morales Claro, Darlan Candido, Lucas A. Moyses Franco, Pamela S. Andrade, Thais M. Coletti, Camila A. M. Silva, Flavia C. Sales, Erika R. Manuli, Renato S. Aguiar, Nelson Gaburo, Cecília da C. Camilo, Nelson A. Fraiji, Myuki A. Esashi, "Genomic characterisation of an emergent SARS-CoV-2 lineage in Manaus: preliminary findings - SARS-CoV-2 coronavirus / nCoV-2019 Genomic Epidemiology - Virological." .

[97] E. C. Sabino *et al.*, "Resurgence of COVID-19 in Manaus, Brazil, despite high seroprevalence," *Lancet*, vol. 397, no. 10273, pp. 452–455, Jan. 2021, doi: 10.1016/s0140-6736(21)00183-5.

[98] L. F. Buss *et al.*, "Three-quarters attack rate of SARS-CoV-2 in the Brazilian Amazon during a largely unmitigated epidemic," *Science (80-.).*, vol. 371, no. 6526, pp. 288–292, Jan. 2021, doi: 10.1126/science.abe9728.

[99] H. Wang *et al.*, "Mutation-Specific SARS-CoV-2 PCR Screen: Rapid and Accurate Detection of Variants of Concern and the Identification of a Newly Emerging Variant with Spike L452R Mutation," *J. Clin. Microbiol.*, vol. 59, no. 8, Jul. 2021, doi: 10.1128/JCM.00926-21.

[100] C. B. F. Vogels *et al.*, "Multiplex qPCR discriminates variants of concern to enhance global surveillance of SARS-CoV-2," *PLOS Biol.*, vol. 19, no. 5, p. e3001236, May 2021,

doi: 10.1371/JOURNAL.PBIO.3001236.

[101] S. Matsuyama *et al.*, “Enhanced isolation of SARS-CoV-2 by TMPRSS2- expressing cells,” *Proc. Natl. Acad. Sci. U. S. A.*, vol. 117, no. 13, pp. 7001–7003, Mar. 2020, doi: 10.1073/pnas.2002589117.

[102] N. Nao *et al.*, “Consensus and variations in cell line specificity among human metapneumovirus strains,” *PLoS One*, vol. 14, no. 4, Apr. 2019, doi: 10.1371/journal.pone.0215822.

[103] V. M. Corman *et al.*, “Detection of 2019 novel coronavirus (2019-nCoV) by real-time RT-PCR,” *Eurosurveillance*, vol. 25, no. 3, p. 2000045, Jan. 2020, doi: 10.2807/1560-7917.ES.2020.25.3.2000045.

[104] D. Svec, A. Tichopad, V. Novosadova, M. W. Pfaffl, and M. Kubista, “How good is a PCR efficiency estimate: Recommendations for precise and robust qPCR efficiency assessments,” *Biomol. Detect. Quantif.*, vol. 3, p. 9, Mar. 2015, doi: 10.1016/J.BDQ.2015.01.005.

[105] “nCoV-2019 sequencing protocol v2 (GunIt).” .

[106] “nCoV-2019 sequencing protocol v3 (LoCost).” .

[107] J. R. Tyson *et al.*, “Improvements to the ARTIC multiplex PCR method for SARS-CoV-2 genome sequencing using nanopore,” *bioRxiv*, vol. 3. bioRxiv, p. 1, Sep. 2020, doi: 10.1101/2020.09.04.283077.

[108] “Artic Network ncov2019-bioinformatics-sop.” .

[109] A. Rambaut *et al.*, “A dynamic nomenclature proposal for SARS-CoV-2 lineages to assist genomic epidemiology,” *Nat. Microbiol.*, vol. 5, no. 11, pp. 1403–1407, Nov. 2020, doi: 10.1038/s41564-020-0770-5.

[110] F. Wu *et al.*, “A new coronavirus associated with human respiratory disease in China,” *Nature*, vol. 579, no. 7798, pp. 265–269, Mar. 2020, doi: 10.1038/s41586-020-2008-3.

[111] “(No Title).” .

[112] R. K. Gupta, “Will SARS-CoV-2 variants of concern affect the promise of vaccines?,”

Nature Reviews Immunology, vol. 21, no. 6. Nature Research, pp. 340–341, Apr. 2021, doi: 10.1038/s41577-021-00556-5.

[113] G. Dudas *et al.*, "Travel-driven emergence and spread of SARS-CoV-2 lineage B.1.620 with multiple VOC-like mutations and deletions in Europe 3," *Sylvie Behillil*, vol. 15, p. 2021.05.04.21256637, May 2021, doi: 10.1101/2021.05.04.21256637.

[114] "Threat Assessment Brief: Emergence of SARS-CoV-2 B.1.617 variants in India and situation in the EU/EEA." .

[115] N. Matic *et al.*, "Early Release - Rapid Detection of SARS-CoV-2 Variants of Concern, Including B.1.1.28/P.1, in British Columbia, Canada - Volume 27, Number 6—June 2021 - Emerging Infectious Diseases journal - CDC," doi: 10.3201/EID2706.210532.

[116] S. Haim-Boukobza *et al.*, "Detecting Rapid Spread of SARS-CoV-2 Variants, France, January 26–February 16, 2021," *Emerg. Infect. Dis.*, vol. 27, no. 5, May 2021, doi: 10.3201/eid2705.210397.

[117] R. da S. Francisco *et al.*, "Pervasive transmission of E484K and emergence of VUI-NP13L with evidence of SARS-CoV-2 co-infection events by two different lineages in Rio Grande do Sul, Brazil," *Virus Res.*, vol. 296, p. 198345, Apr. 2021, doi: 10.1016/j.virusres.2021.198345.

[118] E. Meibalan and M. Marti, "Biology of Malaria Transmission," *Cold Spring Harb. Perspect. Med.*, vol. 7, no. 3, p. a025452, Mar. 2017, doi: 10.1101/cshperspect.a025452.

[119] World Health Organization, *World Malaria Report 2020*. Geneva, 2020.

[120] J. Landier *et al.*, "The role of early detection and treatment in malaria elimination," *Malar. J.*, vol. 15, no. 1, p. 363, Dec. 2016, doi: 10.1186/s12936-016-1399-y.

[121] S. Picot, M. Cucherat, and A.-L. Bienvenu, "Systematic review and meta-analysis of diagnostic accuracy of loop-mediated isothermal amplification (LAMP) methods compared with microscopy, polymerase chain reaction and rapid diagnostic tests for malaria diagnosis," *Int. J. Infect. Dis.*, vol. 98, pp. 408–419, Sep. 2020, doi: 10.1016/j.ijid.2020.07.009.

[122] M. Gatton, "Methods Manual," *World Heal. Organ.*, no. 1, pp. 1–109, 2012.

[123] S. Das *et al.*, “Performance of an ultra-sensitive Plasmodium falciparum HRP2-based rapid diagnostic test with recombinant HRP2, culture parasites, and archived whole blood samples,” *Malar. J.*, vol. 17, no. 1, p. 118, Dec. 2018, doi: 10.1186/s12936-018-2268-7.

[124] L. Ochola, P. Vounatsou, T. Smith, M. Mabaso, and C. Newton, “The reliability of diagnostic techniques in the diagnosis and management of malaria in the absence of a gold standard,” *Lancet Infect. Dis.*, vol. 6, no. 9, pp. 582–588, Sep. 2006, doi: 10.1016/S1473-3099(06)70579-5.

[125] A. Bosman, J. Cunningham, K. A. Lindblade, and A. Noor, “WHO Technical Consultation on research requirements to support policy recommendations on highly sensitive malaria diagnostic tests,” *World Malar. Rep.*, no. October, pp. 1–34, 2018, [Online]. Available: https://www.who.int/malaria/mpac/mpac-april2018-hi-sensitive-tests-session5.pdf.

[126] J. M. Roth, D. A. Korevaar, M. M. G. Leeflang, and P. F. Mens, “Molecular malaria diagnostics: A systematic review and meta-analysis,” *Crit. Rev. Clin. Lab. Sci.*, vol. 53, no. 2, pp. 87–105, Mar. 2016, doi: 10.3109/10408363.2015.1084991.

[127] M. C. Mwenda *et al.*, “Performance evaluation of RDT, light microscopy, and PET-PCR for detecting Plasmodium falciparum malaria infections in the 2018 Zambia National Malaria Indicator Survey,” *Malar. J.*, vol. 20, no. 1, p. 386, Dec. 2021, doi: 10.1186/s12936-021-03917-6.

[128] A. Amir, F.-W. Cheong, J. R. De Silva, and Y.-L. Lau, “Diagnostic tools in childhood malaria,” *Parasit. Vectors*, vol. 11, no. 1, p. 53, Dec. 2018, doi: 10.1186/s13071-018-2617-y.

[129] K. Zainabadi *et al.*, “A novel method for extracting nucleic acids from dried blood spots for ultrasensitive detection of low-density Plasmodium falciparum and Plasmodium vivax infections,” *Malar. J.*, vol. 16, no. 1, p. 377, Dec. 2017, doi: 10.1186/s12936-017-2025-3.

[130] E. A. Guirou *et al.*, “Molecular malaria surveillance using a novel protocol for extraction and analysis of nucleic acids retained on used rapid diagnostic tests,” *Sci. Rep.*, vol. 10, no. 1, p. 12305, Dec. 2020, doi: 10.1038/s41598-020-69268-5.

[131] E. Kamau, S. Alemayehu, K. C. Feghali, D. Saunders, and C. F. Ockenhouse, “Multiplex qPCR for Detection and Absolute Quantification of Malaria,” *PLoS One*, vol. 8, no. 8, p.

e71539, Aug. 2013, doi: 10.1371/journal.pone.0071539.

[132] T. Schindler *et al.*, "Molecular monitoring of the diversity of human pathogenic malaria species in blood donations on Bioko Island, Equatorial Guinea," *Malar. J.*, vol. 18, no. 1, p. 9, Dec. 2019, doi: 10.1186/s12936-019-2639-8.

[133] T. Schindler *et al.*, "A multiplex qPCR approach for detection of pfhrp2 and pfhrp3 gene deletions in multiple strain infections of Plasmodium falciparum," *Sci. Rep.*, vol. 9, no. 1, p. 13107, Dec. 2019, doi: 10.1038/s41598-019-49389-2.

[134] J. B. Munro, C. G. Jacob, and J. C. Silva, "A Novel Clade of Unique Eukaryotic Ribonucleotide Reductase R2 Subunits is Exclusive to Apicomplexan Parasites," *J. Mol. Evol.*, vol. 77, no. 3, pp. 92–106, Sep. 2013, doi: 10.1007/s00239-013-9583-y.

[135] D. J. Padley, A. B. Heath, C. Sutherland, P. L. Chiodini, and S. A. Baylis, "Establishment of the 1st World Health Organization International Standard for Plasmodium falciparum DNA for nucleic acid amplification technique (NAT)-based assays," *Malar. J.*, vol. 7, no. 1, p. 139, Dec. 2008, doi: 10.1186/1475-2875-7-139.

[136] K. A. Fleming *et al.*, "The Lancet Commission on diagnostics: transforming access to diagnostics," *Lancet*, Oct. 2021, doi: 10.1016/S0140-6736(21)00673-5.

[137] U. Dalrymple, R. Arambepola, P. W. Gething, and E. Cameron, "How long do rapid diagnostic tests remain positive after anti-malarial treatment?," *Malar. J.*, vol. 17, no. 1, p. 228, Dec. 2018, doi: 10.1186/s12936-018-2371-9.

[138] S. Hosch *et al.*, "Analysis of Nucleic Acids Extracted from Rapid Diagnostic Tests Reveals a Significant Proportion of False Positive Test Results Associated with Recent Malaria Treatment," *SSRN Electron. J.*, pp. 1–36, 2021, doi: 10.2139/ssrn.3839416.

[139] W. Johannsen, *Elemente der exakten erblichkeitslehre. Deutsche wesentlich erweiterte ausgabe in fünfundzwanzig vorlesungen, von W. Johannsen.* Jena,: G. Fischer, 1909.